Single-grain OSL dating of Welsby Lagoon, Queensland:

Bridging Australia's MIS 3 Gap

Thesis submitted in accordance with the requirements of the University of Adelaide for an Honours Degree in Geology/Geophysics

Richard John Lewis

November 2015

THE UNIVERSITY of ADELAIDE

SINGLE-GRAIN OSL DATING OF WELSBY LAGOON, QUEENSLAND

BRIDGING AUSTRALIA'S MIS 3 GAP

ABSTRACT

Marine Isotope Stage 3 (MIS3: ~29 – 57 ka) is an important period in Australian prehistory as it contains the key events of human arrival and megafauna extinction. A firm understanding of palaeoenvironmental conditions during this period is needed to disentangle the relationship between these events and climatic change. However, there are currently few palaeoenvironmental records in Australia which detail this period and which have reliable chronological constraints. This study examines a new sedimentary record from Welsby Lagoon, North Stradbroke Island, which has the potential to advance our understanding of MIS3 climate change in eastern Australia. The study explores the feasibility of applying single-grain optically stimulated luminescence (SG-OSL) in subtropical Queensland's Welsby Lagoon, as a means of constraining a key paleoenvironmental record spanning MIS 3. Specifically, the study aims to establish the dateability of Welsby Lagoon using OSL, create an age-depth model and assess the continuity of the sedimentary record. OSL provides direct age constraints on sediment depositional events and is able to surpass the age constraints and assumptions of conventional radiocarbon (14C) dating. SG-OSL dating is applied to 5 lacustrine and 4 basal sand samples from Welsby lagoon. These results are combined within a Bayesian framework to produce two continuous age-depth models extending to at least MIS 4 at 83.4-70.4 ka (2σ confidence interval) for Welsby Lagoon. Statistical analyses of grain populations, through OSL and sedimentology, suggest aeolian forcing as the primary grain transportation mechanism, with sourcing primarily from local dunes. Geochemical data obtained through ITRAX scanning and correlation with the age-depth models identifies a continuous sedimentation history which, in conjunction with the ability to date the sedimentary record using OSL, identifies Welsby Lagoon as potentially one of the most highly resolved and robustly dated pre-MIS 2 records in eastern Australia. Studies such as this are essential for understanding climate systems during an important period of palaeoecological change in Australian prehistory.

KEYWORDS

OSL dating, single-grain, Welsby Lagoon, North Stradbroke Island, multi-gran, MIS 3

TABLE OF CONTENTS

LIST OF FIGURES

LIST OF TABLES

INTRODUCTION

In the Southern Hemisphere there is currently a lack of high resolution, well dated, continuous terrestrial sedimentary records which cover a full glacial/interglacial cycle (Voelker 2002, Ganopolski and Roche 2009). Consequently, it is difficult to establish the effect of Northern Hemisphere climatic events, such as Dansgaard-Oeschger and Heinrich events, on Southern Hemisphere environments as a result to changes in the thermohaline circulation (Barbante *et al.* 2006, Muller *et al.* 2008, Thomas *et al.* 2009,

Chiang and Friedman 2012). Lack of knowledge about Southern Hemisphere climates also convolutes the controversial discussion on the driver of megafauna extinction in Australia during marine isotope stage (MIS) 3 (57–29 ka), with hypothesises including human induced environmental changes and climate instability (Kershaw 1986, Flannery 1990, Cohen *et al.* 2015).

Much of the current understanding of MIS 3 climates in eastern Australia comes from pollen and charcoal data primarily from Lynch's Crater (Turney *et al.* 2006, Muller *et al.* 2008, Rieser and Wüst 2010) and Caledonia Fen (Kershaw 1986, 2010, Roberts *et al.* 2003). These records rely heavily on age-depth models incorporating only radiocarbon dating in lakes, environments noted to be difficult to date with this method due to carbon recycling (Bowler *et al.* 1986, Blaauw *et al.* 2004). Notably, both these sites show a change to a more arid environment at interglacial/glacial transitions. This has resulted in debate about the onset of ecological change throughout Australia's east coast at local scales. For example a change to a more arid environment could be explained by Aboriginal burning (Kershaw 1974, 1986), or by increased fuel via vegetation overgrowth related to megafauna extinction (Flannery 1990, Lopes dos Santos *et al.* 2013). Another hypothesis is that change may be due to climactic variability (Murphy *et al.* 2012, Cohen *et al.* 2015) leading to growth of more fire susceptible vegetation. Welsby Lagoon, on North Stradbroke Island, Queensland, is situated in the subtropical region mid-way between Lynch's Crater and Caledonia Fen. However, the value of the Welsby Lagoon sediment record as an archive of environmental change will depend on whether the sequence is continuous, if it can be dated beyond the limits of radiocarbon and if an age model can be developed.

This paper will establish the feasibility of implementing conventional multi-grain and single-grain OSL dating in Welsby Lagoon through statistical analysis of single grain populations (Galbraith and Green 1990, Galbraith *et al.* 1999, Galbraith 2003). It will also produce age-depth models for the Welsby Lagoon record using OSL dating of the lagoonal and basal sand sediments, extending the current age model past the previous of radiocarbon age of 28 ka by Moss *et al.* (2013). Finally, this paper will also establish if the core is continuous through the correlation of chronological controlled age-depth models, elemental compositions and grain size.

BACKGROUND

North Stradbroke Island History

North Stradbroke Island is located ~40 km east of Brisbane (Figure 1) and is the second largest sand island in the world (after Fraser Island). The approximate 35 km length of the island is orientated in an N-NE to S-SW direction, with a width ranging from 2 to 11 km (Thompson 1992). Studies by Kelley and Baker (1984), Tejan-Kella *et al.* (1990), found that the island's composition is predominantly sand deposits, lithified sedimentary, meta-sedimentary and volcanic units.

The climate of North Stradbroke Island is classified as subtropical, with mild, dry winters and warm, moist summers (Clifford and Specht 1979, Colls and Whitaker 1990, Thompson 1992, Moss *et al.* 2013). The Pacific trade winds dominate the south-easterly wind direction meanwhile the island experiences average annual rainfall of ~1500 mm/year (Clifford and Specht 1979, Thompson 1992).

Preliminary strudies by Pickett *et al.* (1985) on coral found that the formation of North Stradbroke Island pre-dates MIS 5e (123-109 ka; $^{230}Th/^{234}U$). This is supported by Ward

(2006) who concluded that the island formation was as early as MIS 11 (460 ka; OSL). MIS 11 (424-734 ka) is noted as a particularly long interglacial period by Loutre and Berger (2003) following the extended glacial MIS 12 (478–424 ka). This time period encompasses sea level fluctuation leading to the hypothesis that the dunes were aeolian in origin (Ward 2006, Brooke *et al.* 2008). The average height of the dunes on North Stradbroke Island range from ~100 m to ~150 m, and the highest point is 239 m above sea level.

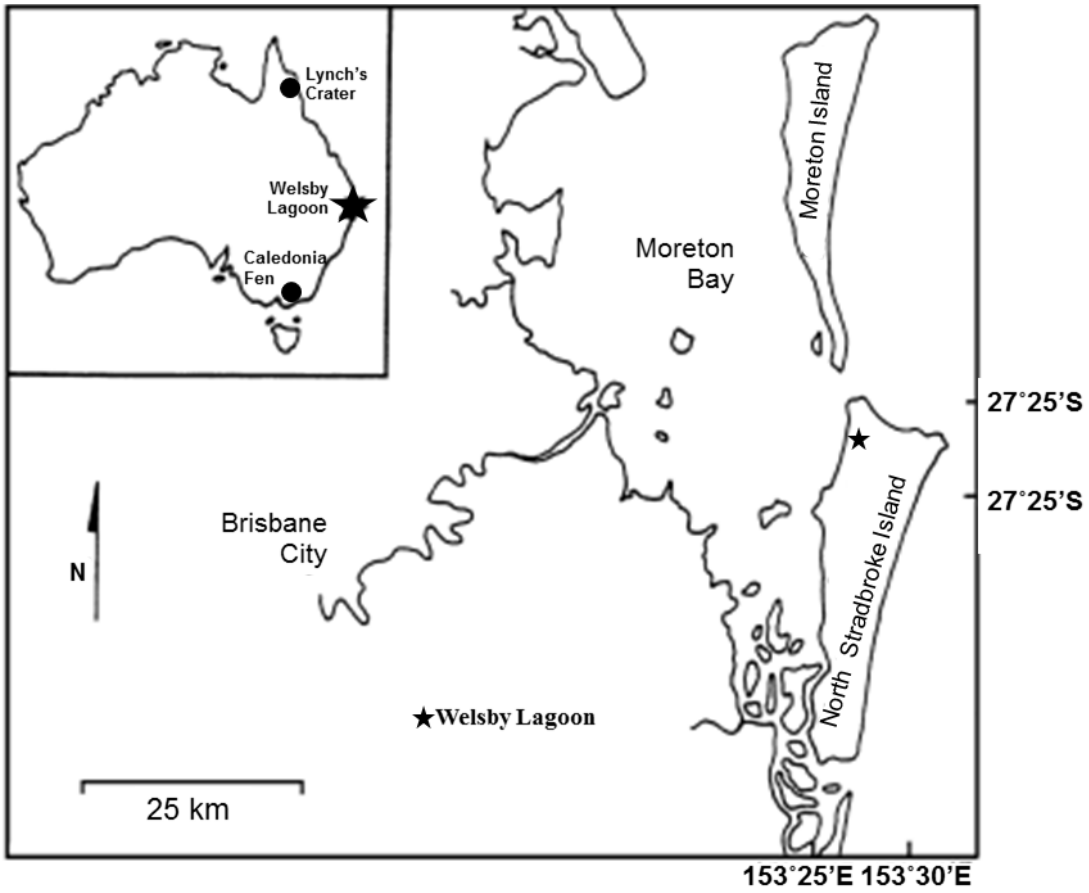

Figure 1: Map showing the location of subtropical Welsby Lagoon in south-eastern Queensland, Australia. The inset map shows the study sites location with respect to alpine Caledonia Fen and tropical Lynch's Crater. Adapted from (Mosisch and Arthington 2001).

Marine Isotope Stage 3

MIS 3 is a period spanning an estimated 28 ka between 57–29 ka. This was a period of low $\delta^{18}O$ in deep sea cores related to warmer interglacial conditions. This is an

important time period globally because there was substantial climatic variability and rapid climate changes. MIS 3 is particularly important to Australia because this was also a time of human arrival and megafaunal extinction. Developing paleoclimate data is important in Australia in order to examine the relative impacts of climate and humans in regards to the extinction of megafauna

GLOBAL MIS3

Globally MIS 3 is important as Greenland ice records show the period hosts frequent climactic fluctuations with temperate changes of up to 15˚C in 10 years (Thomas *et al.* 2009, Wolff *et al.* 2010). These abrupt climate transitions from cold (stadial) conditions to mild (interstadial) conditions, eventually followed by a return to cold conditions, are known as a Dansgaard-Oeschger (DO) events (Dansgaard *et al.* 1993). The causes of these DO events is debated, however Yang and Neelin (1993) suggest that changes to the strength of the Thermohaline Circulation (THC), a movement of ocean temperature and salinity across gradients, may be a driving mechanism. A weak THC state is associated with stadials, while strong THC is associated with interstadials.

Changes in the THC leading to DO events are hypothesised to be associated with massive iceberg surges originating from the Laurentide Ice Sheet, known as Heinrich events (Heinrich 1988). MIS 3 hosts Heinrich events 3–6, however like the DO events, there is still uncertainty with what caused the ice sheet breakup (Broecker *et al.* 1992). It should be noted that the uncertainty in the causes of DO and Heinrich events is related to the low resolution and sparse continuous records in the southern hemisphere (Ganopolski and Roche 2009).

Discovering more Southern Hemisphere records is also important to explore the antiphase hemispherical relationship, where cooling in the North Atlantic results in warming in the Antarctic (Barbante *et al.* 2006), known as the "bipolar seesaw" along the THC. Once again the current low resolution chronologies in the south restrict the comparison of hemispherical forcing and response (lead and lag) events associated with glacial/interglacial cycles on regional scales (Ganopolski and Roche 2009). The lack of comparable local Australasian records makes it difficult to differentiate between proxy signals recording global climate change or a modified signal due to influences such as El Niño Southern Oscillation (Kershaw *et al.* 2003).

AUSTRALIA'S MIS 3

MIS 3 is a particularly important time period for Australia as human arrival coincided with the extinction of ~90% of megafauna between 48.9 ka and 43.6 ka (1σ confidence level), the so-called Late Quaternary megafauna extinction (LQME) (Lopes dos Santos *et al.* 2013). Uncertainty in the degree which fire regime changes, climate variability and human-megafauna interactions had on driving the LQME are still debated. Changes in the fire regime have been investigated with charcoal records. There are several hypothesis for the fluctuations in the charcoal records in Australia, including landscape alteration due to burning by Aboriginal people and increased burning material. At Lynch's Crater Kershaw (1974), first suggested that Aboriginal burning had led to a sustained decline in fire-sensitive vegetation. Meanwhile Flannery (1990) proposed that megafaunal extinction brought about by over-hunting by humans lead to vegetation overgrowth and increased fuel loads, thereby increasing burning. Interestingly, using the charcoal record at Lynch's Crater, Rule *et al.* (2012) suggested that the increase in charcoal resulted from less grazing pressure by megafauna, shown

with a decrease in fungi associated with megafaunal dung, thereby supporting Flannery (1990). However it should be noted that the variations in the fire regime, and therefore charcoal record, may occur without association with humans (Mooney *et al.* 2011). Situations such as this may be induced though climactic variance causing drying, or favourable conditions for fire prone vegetation, which may also explain the aforementioned events. Recently, Cohen *et al.* (2015) addressed the change in C4 to C3 vegetation, seen in the $\delta^{13}C$ in egg shells of *Dromaius novaehollandiae* and *Genyornis newtoni* (Miller *et al.* 1999) around Lake Eyre. Producing chronological controls on the formation of palaeo-shorelines using OSL, he found that climactic variance played a larger role on vegetation changes than has been previously accepted.

Investigation into the climatic variability/stability in Australia has involved the reconstruction of pollen records. Two predominant sites of eastern Australia with such records include Lynch's Crater and Caledonia Fen. Studies by Kershaw (1976) investigated the pollen record at Lynch's Crater highlighting that there was an increase in aridity, as forest vegetation is replaced by savanna grasses. Changes in vegetation communities at Caledonia Fen also support the initiation of drier conditions at the conclusion of MIS 3 (Kershaw *et al.* 2007). Together these pollen records indicate that most of eastern Australia experienced a climatic trend towards drier conditions (Kershaw *et al.* 2003, Hesse *et al.* 2004, Turney *et al.* 2006). However, this change towards a drier more variable climate in the Southern-Hemisphere has not resulted in wetting in the Northern-Hemisphere as would be expected by the antiphase hemispherical relationship. The difficulties of correlating these changes with global records arises from the lack of reliable chronologies.

Statements above show that there are many interpretations for how records change and distinguishing between forcing factors is difficult. Opposing interpretations arise from contesting the reliability of dating through radiocarbon alone.

The argument behind the reliability of radiocarbon alone for age-depth models in lacustrine sediments is that is can over or underestimate timing of sediment deposition. This arises when depleted ^{14}C is incorporated into lake sediments through dissolution or transportation, along with mis-interpretation of the dated material's association with the sediments (Björck and Wohlfarth 2001, Walker *et al.* 2007).

Dating the timing of sediment deposition is crucial for identifying an ecosystem's response to environmental changes across broad ranges of timescales. The dating of geological and archaeological events would be easier if the mineral grains contained within the sediment could be dated independently, without having to make assumptions about the minerals relationship with the specific horizon (Huntley *et al.* 1987). OSL dating has been accepted as a method capable of producing this result while also increasing the age range of models from ~50 ka (radiocarbon) to ~250 ka. Currently in eastern Australia, OSL dating has been adopted to refine the age depth models in Lynch's Crater and Caledonia Fen (Table 1). However despite the importance of these sites, more dated sites are needed to understand factors driving climate change. This is also translated to subtropical Australia where fewer chronological constraints are in place with respect to its temperate counterparts due to lack of known datable sites. However, with the discovery of Welsby Lagoon on the sandy North Stradbroke Island the spatial and chronological gap will bridged.

Table 1: Optically stimulated luminescence ages constraints for known sediment records in Eastern Australia which span a glacial/interglacial transition before human arrival. Lynch's Crater data sourced from Rieser and Wüst (2010). Caledonia data sourced from Kershaw *et al.* (2007).

Optically stimulated luminescence ages obtained at Australian sites, Lynch's Crater and Caledonia Fen.		
Lynch's Crater		
Depth (cm)	Age (ka)	MIS[a]
1660	181.5±62.7	6
2410	60.7±11.0	4
2860	79.2±10.9	5a
3350	103.4±13.5	5c
3950	122.7±22.7	5e
4400	138.0±17.1	6
5000	159.7±26.8	6
5600	156.7±23.5	6
Caledonia Fen		
Depth (cm)	Age (ka)	MIS[a]
748–755	66±8	4
776–783	68±8	4

[a] Marine Isotope Stage
[b] Optically Stimulated Luminescence Dating

Study Site

Welsby lagoon, North Stradbroke Island, forms within a perched water table at an altitude of ~21 m. Surrounded by dunes, sediment at Welsby Lagoon has accumulated in the water filled depression overlaying an impermeable layer. Timms (1986) described the impermeable layer as forming through the precipitation of organic and inorganic matter in the soil profile, resulting from chemical reactions between soil and water. Previous radiocarbon dating from the outer edges of the water line in a 4.5 m core produced a basal age of 28 ka (Moss *et al.* 2013). This suggests that the extracted 12 m core of this study would be much older contains many MIS stages.

The transport of most of the modern coastal siliceous sand in south-eastern Queensland is from the south, predominantly driven by south-easterly currents and wind regimes (Ward 1978, Ward 2006). Currently aeolian forcing is considered to be the main driver of sedimentation across North Stradbroke Island and coastal eastern Australia (Petherick *et al.* 2011, Lamy *et al.* 2014). This suggests that the quartz within the Welsby Lagoon sediment would have primarily been sourced from the local surrounding dunes. Studies by Tejan-Kella *et al.* (1990), Thompson (1992), Thompson and Bowman (1984) on the local dune fields of eastern Queensland found the modal grain size to be between 180–250μm.

OSL Dating

Radiocarbon dating has conventionally been utilised for determining the age of a variety of organic materials in Quaternary deposits in Australia (Baker *et al.* 1985, Bowler *et al.* 1986, Ramsey 1995, Gillespie 1997). However, the short half-life of ^{14}C dictates the accuracy and reliability of the method is limited to within 50 ka (Blaauw *et al.* 2004). Optically stimulated luminescence (OSL) dating overcomes the age limitations and

assumptions of radiocarbon dating, extending the datable age range of datable sediments to 250 ka. Furthermore, numerical ages produced with OSL requires no subsequent calibration (Lian and Roberts 2006, Wintle and Murray 2006). OSL dating records the mineral grain's most recent exposure to sunlight or heating, thereby indicating time of deposition.

The natural luminescence signal within minerals such as quartz develops through exposure to ionizing radiation. The mineral lattice is prone to defects (traps; Refer to Appendix A for definitions of OSL dating nomenclature) in which ionizing radiation in the form of alpha (α), beta (β), gamma (γ), and cosmic radiation (from the decay series of potassium, thorium and uranium in the sediment) can dislocate charges and store them. The charges can reside in the defects from seconds to millions of years. As irradiation continues to displace charges, the traps become progressively filled until reaching saturation point, only to be released on exposure to daylight or heating (Huntley *et al.* 1987).

Through measuring the amount of dislocated charge and incorporating knowledge of incident radiation over time, the depositional age of a quartz grain can be calculated (i.e. its last exposure to daylight or heat). This is achieved though the equation:

$$Age\ [ka] = \frac{equivalent\ dose\ (D_e)}{dose\ rate}\ \frac{[Gy]}{[Gy/\mathrm{ka}]}$$

Where the equivalent dose (D_e) is the laboratory equivalent of the total radiation dose absorbed by the sample during burial (amount of displaced charges) and the 'dose rate' is the rate at which the dose was imparted to the sample through ionizing radiation exposure to isotopes in the decay series' of ^{40}K, ^{238}U, ^{235}U, ^{232}Th and cosmic rays. Typically, single and multi-grain quartz aliquots are prepared under subdued red light conditions when evaluating the D_e through OSL signal measurement. The necessity of

these preparation conditions is because the D_e signal is diminished with light exposure leading to resetting (bleaching) of the OSL dating 'clock' (Aitken 1998, Duller 1991). In the laboratory the natural signal is measured, followed by a series of signal measurements in response to varying known irradiation doses (regen dose). Each OSL measurement is followed by a second OSL measurement using a constant dose (test dose) to assess sensitivity changes in the quartz. The normalisation of the measured luminescence signal with the test dose allows the construction of a dose response curve. From this curve the D_e associated with the natural signal can be interpreted (Figure 2).

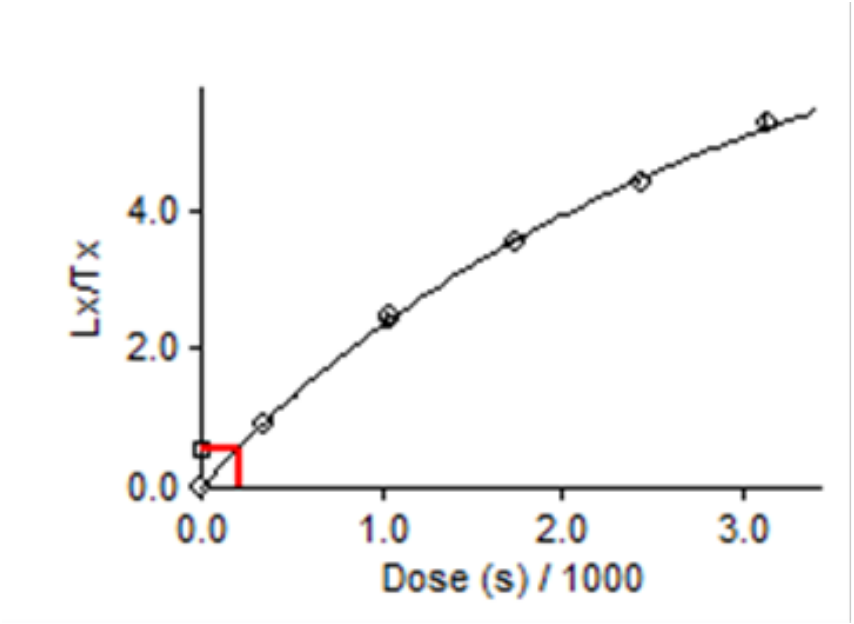

Figure 2: An example of a dose response curve used for interpretation of the D_e associated with a natural dose. The vertical axis shows normalised optically stimulated luminescence photon counts between the respective regen doses and test doses (L_x/T_x). The horizontal axis shows the amount of dose given. The diamonds represent the series of measurements made with varying doses to construct the dose curve. The red lines show the interpolation of the natural luminescence signal to obtain the respective D_e (seconds/1000).

Traditional OSL dating techniques involve the use of multi-grain age estimates in which an average equivalent dose response from many grains is taken. This can lead to equivalent dose (D_e) miscalculations in complex sedimentary systems where insufficient exposure to light or heat does not reset stored signals to zero (partial bleaching) and/or

mixing has occurred (Duller 1991, Bateman et al. 2003, Arnold and Roberts 2009). Notably the ability to measure the D_e of a single grain, along with the incorporation of site-specific information and statistical analytical techniques (Galbraith et al. 1999, Duller 2008, Arnold and Roberts 2009), means the 'masking' effect of multiple grain analysis can be overcome. The drawback of using single-grain over multi-grain analysis for completely bleached, undisturbed quartz populations is one of measurement time (days vs hours). This is due to machine run time increase with single-grain measurements and the increased time associated with manual analysis of larger D_e datasets. The end result of using single-grain or multi-grain analysis in simple depositional environments is that both methods will produce similar D_e values, grain populations, and therefore ages.

As North Stradbroke Island is a sand island, there is the opportunity to utilise OSL dating of quartz grains to produce a direct deposition chronology. The focus of this will be on developing a chronology through what is suspected to be the MIS3 record and the basal sands of Welsby Lagoon. OSL single-grain dating will allow assessment of any erosional features such as unconformities in the sediments, thereby testing the hypothesis of continuous sedimentation at Welsby Lagoon. Furthermore, through statistical analysis of the OSL ages and grain data, this paper aims to identify grain population characteristics eluding to the transport mechanisms of the lacustrine sediments, and thereby assess the feasibility of implementing multi-grain (or single-grain) OSL at similar sites in future studies.

METHODS

Field and Coring

The location of coring was in the centre of Welsby Lagoon as to minimise the likelihood of sampling sediment which has wetted and dried over time due to lake level flux as observed on the outer edges. Sediment was extracted from two, 0.5 m offset, parallel cores, WL15/1 and WL15/2, extending down to 12.78 m and 12.72 m respectively (Table 2). The coring process involved minimalizing sediment exposure to light by using black PVC tubing coupled to a modified Bolivia corer (Myrbo and Wright 2008). Once raised, the 1m core sections were wrapped in black plastic to maintain the integrity of the natural luminescence signal so OSL dating could be conducted in the laboratory.

Table 2: Details measurements taken from parallel sediment cores WL15/1 and WL15/2 from Welsby Lagoon, North Stradbroke Island.

Welsby Lagoon core information		
Coring Date	16th March 2015	
Coring location	S 27.43646, E 153.44893	
Elevation[c]	29.063 m	
Lake Area [a]	151656 m^2	
Core ID	WL15/1	WL15/2
Core length (cm)	1278.0	1272.3
Sediment Density	0.99–1.62 g/cm^3	
Water Content	1094.0–89.1%[b]	
	n=103, mean=642.55%[b]	
Inorganic Content	0.13–98.43%[b]	
	n=101, mean=29.3%[b]	
Organic Content	1.57–99.87%[b]	
	n=101, mean=70.70%[b]	

[a] approximate size based on google earth 2015.
[b] expressed as percentage of dry sample weight.
[c] above modern-day sea-level.

Loss on Ignition

The 100 cm sediment core drives were split under subdued red light in the Prescott Environmental Luminescence Laboratory at The University of Adelaide. Water content, bulk density and organic matter content was measured by weight loss on ignition (LOI). 1 cm^3 samples were taken down core at 10 cm intervals in core WL15/2, except for the basal sediments where the resolution increased to 8 cm due to observed sediment change. These samples were dried at 105˚C to obtain water content followed by combustion at 550˚C for 18 hours, to measure organic and inorganic matter, using a modified method of Heiri *et al.* (2001). The measured water content values from LOI were used to establish a water content-depth relationship to reconstruct water loss through compaction as outlined by Athy (1930).

Archive cores from Welsby Lagoon were analysed at 1 mm resolution for magnetic susceptibility and elemental abundance at Australian national nuclear research and development organisation (ANSTO) using an Itrax core logger.

OSL Preparation

The procedure for obtaining a single OSL date from quartz grains is a time-intensive process which requires a lengthy preparation stage followed by extensive analysis of individual single-grains (Figure 3). Furthermore the preparation must be carried out in strictly subdued red light conditions (λ>590nm) to prevent contamination of the light sensitive samples. For this project preparation and measurements were undertaken in the specially equipped Prescott luminescence laboratories at The University of Adelaide.

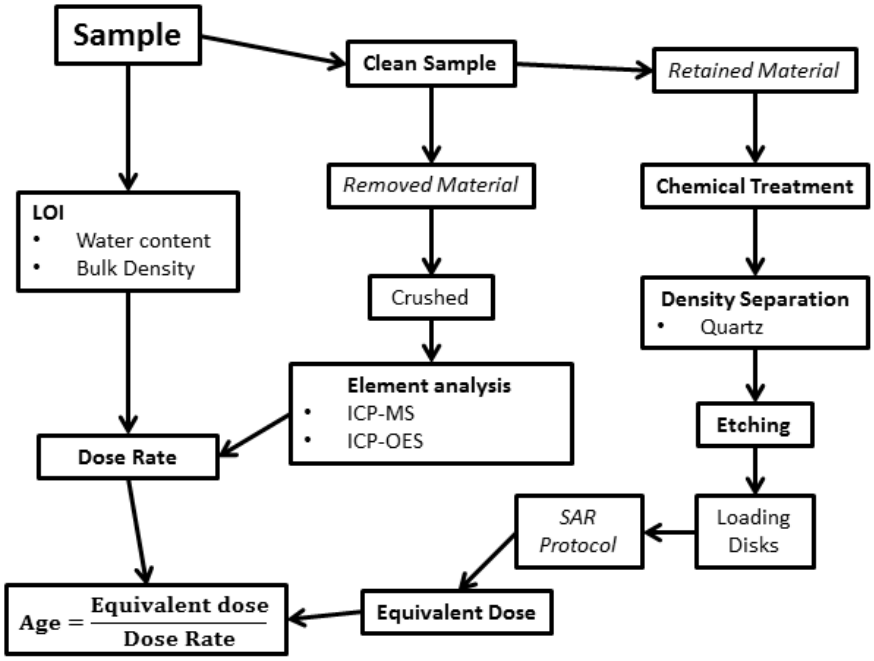

Figure 3: Preparation steps involved in optically stimulated luminescence age dating.

SAMPLE EXTRACTION FROM CORE

The extraction of seven samples were taken between 350 cm and 850 cm in an attempt to capture the timing of MIS 3, and two were taken from the basal sediments to determine the age of the entire sequence and timing of lake formation (Table 3). The size of sediment sample removed from the core varied between 20 cm, 10 cm and 1 cm based on judgement of quartz content at a given depth (using the fraction remaining after ignition at 550˚C).

Extracting the samples from the core required the removal of any material which may have been disturbed or exposed to light during the coring and/or transportation process. This was achieved by removing 5–8 mm of material from the split core surface and any surface in contact with the PVC tubing. The removed material for each sample was retained for dose rate analysis (See Dose Rate Calculations).

Table 3: Optically stimulated luminescence sample resolution for Welsby Lagoon. The sample sizes were based on the amount of inorganic remains after combustion of 1 cm^3 of sediment corresponding to a particular depth at 550˚C for 18 hours.

Samples taken from parallel Welsby Lagoon cores for optically stimulated luminescence age analysis.		
WL15/2		
ID	Depth (cm)	Sample size (cm)
2.3	380	20
2.5	480	20
2.7	580	20
2.9	675	10
2.11	775	10
2.12	815	10
2.2	1258	1
2.1	1270	1
WL15/1		
ID	Depth (cm)	Sample size (cm)
1.6	1258	1
1.7	1270	1

QUARTZ PURIFICATION AND TREATMENT

Samples within the lagoonal sediments were treated with 10% sodium hydroxide to disperse clay aggregates. Each sample was then individually wet sieved using a nest of 355, 250, 212, 180, 125, 90, 63 μm sieves. Size fractions smaller than 63 μm were captured and allowed a minimum of 15 minutes to settle out of suspension before excess water was decanted. All the sieved fractions were then treated with hydrochloric acid (30%) and hydrogen peroxide (30%) to dissolve remaining carbonates and organic material respectively, following the procedure of Aitken (1998). Fractions were then weighed to assess the grain size populations at each depth.

The grain sizes targeted for OSL analysis were the 212–250 μm fraction. However for samples with low quartz yields of this particular fraction, the chosen grain size was revised to 180–250 μm. Density separation (using sodium polytungstate with densities of 2.62 and 2.72 g/cm^3) was conducted on each fraction intended for D_e measurement to separate heavy minerals and feldspars from the quartz. The purified quartz fractions were treated with hydrofluoric acid (etching) to avoid age underestimation which may originate from non-removal of the α-irradiated outer rinds of each grain. Multi-grain runs (~1000 grains) were produced by mounting grains on stainless steel disks (diameter of 1 cm) according to Duller (2008) using silicone oil spray. Single-grain runs required 100 individual etched quartz grains to be loaded onto aluminium discs (~1 cm diameter) drilled with a 10 x 10 array of chambers, each of 300 μm depth and 300 μm diameter (Bøtter-Jensen *et al.* 2000).

LOADING INTO RISØ

Prepared disks were loaded onto the Risø reader carousel ensuring correct orientation of the disks. The OSL measurements were made on a Risø TL/OSL DA-20 reader using a

green (λ=532nm) laser for optical stimulation with (UV-blue luminesence) emissions detected by an Electron Tubes 9235QA photomultiplier tube fitted with 7.5 mm of Hoya U-340 filter. Laboratory irradiation for regeneration doses was undertaken using mounted $^{90}Sr/^{90}Y$ β sources with known dose rates of 6.6 Gy/min and 1.7 Gy/min. Position corrections were applied to each single-grain well to account for spatial variance under the β source.

Equivalent Dose Measurements

DOSE RECOVERY TEST (DRT)

In order to establish a chronology using the single-aliquot regenerative dose (SAR) protocol of Murray and Wintle (2000) the test dose preheat temperatures for D_e determination needed to be established using a dose recovery test (DRT) (at multi-grain and single-grain resolution). Sample WL2(1) was used, due to large quartz yield, for preheat evaluation for all other samples. Test-dose preheat (PH_2) temperatures ranging between 160 to 220˚C (for 10 seconds) with an interval of 20˚C were tested, using a fixed regenerative dose preheat (PH_1) of 260˚C for 10 seconds, with a heating rate of 5˚C/second (Table 4).

The chosen SAR preheat conditions for multi-grain aliquots were determined to be 260˚C for 10 seconds (regen dose) and 220˚C for 10 seconds (test dose), as the measurements had a mean recovered to given dose (25 Gy) ratio of 1.00±0.03 (Figure 4a), a spread about the expected value of 12.7±9.4% and a mean recycling ratio of 1.01±0.01. The corresponding single grain measurements of 0.97±0.01, 5.2±1.7% and 1.00±0.11, supported the suitability of preheating of 260˚C for 10 seconds (regen-dose) and 220˚C 10 seconds (test dose) to recover the administered dose. Importantly, at the

single-grain scale, all DRT results yield a ratio consistent with the administered dose and a recycling ratio consistent with unity at the 2σ and 3σ uncertainty range (Figure 4b), highlighting the suitability the chosen of preheat conditions.

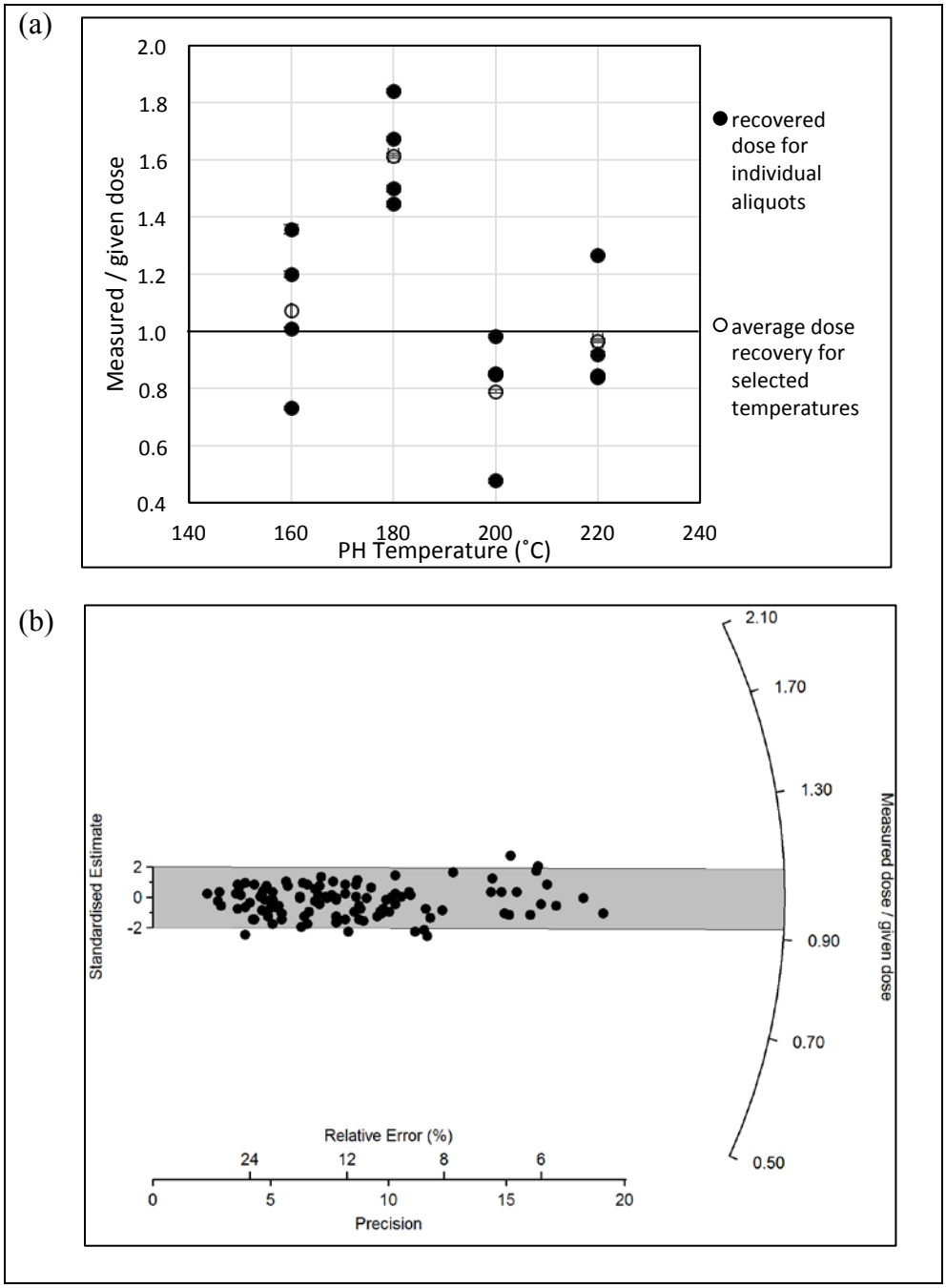

Figure 4: (a) Multi-grain dose recovery test aliquots (each containing ~1000 grains) of sample WL2(1) and their response to preheating conditions 160, 180, 200 and 220˚C after irradiation with 25 Gy. (b) Radial plot of single-grain dose recovery test of sample WL2(1), obtained using the chosen SAR preheats of 260˚C for 10 s (PH1) and of 220˚C for 10 s (PH2). Individual D_e values are displayed as radial plots, where the shaded region on these radial plots is centred on a measured dose to given dose ratio of unity. Individual D_e values that fall within the shaded region are consistent with the given dose at ± 2σ. The over-dispersion value, σ, calculated using the CAM, is shown for single-grain D_e distributions.

MEASURING EQUIVALENCE DOSE

Based on the results of the dose recovery test, all samples were measured on the Risø reader following the SAR protocol shown in Table 4.

The D_e of each single quartz grain samples was calculated using Risø Analyst (Duller 2007) by Monte-Carlo fitting an exponential or exponential plus linear expression to the dose response curve. An additional 2.5% curve reproducibility uncertainty was propogated in quadrature with the D_e uncertainties. Individual grains had to pass all parameters from a rigorous set of rejection criteria before their D_e could be accepted as valid. The rejection criteria are shown in (Table 5).

Table 4: Measurement procedure followed based on the dose recovery test for all Welsby Lagoon samples to obtain equivalence dose values.

Step	Single-grain optically stimulated luminescence single aliquot regenerative dose protocol.	
1[a]	Give dose	
2[b]	Stimulate with infrared diodes at 50 °C for 20 s at 90% power	
3	Preheat to 260 °C for 10 s	
4	Stimulate with green laser at 125 °C for 2 s (90% power)	OSL L_n or L_x
5	Give test dose	
6	Preheat to 220 °C for 10 s	
7	Stimulate with green laser at 125 °C for 2 s (90% power)	OSL T_n or T_x
8	Return to 1	

[a] Step omitted when measuring the natural signal (L_n).
[b] Step added only when measuring the IR depletion ratio described in Duller (2003).

Table 5: Rejection criteria applied to all grains individually to establish if the equivalent dose signal is valid.

	Criteria	Description
1	Weak signals	The net intensity of the natural test-dose signal, T_n[a], was less than three times the standard deviation of the late-light background signal
2	Poor recycling ratios	The ratios of sensitivity-corrected luminescence response (L_x/T_x)[b, c] for two identical regenerative doses were not consistent with unity at 2σ
3	High level signal recuperation	The sensitivity-corrected luminescence response of the 0 Gy regenerative-dose point amounted to more than 5% of the sensitivity-corrected natural signal response (L_n/T_n)[a, d] at 2σ
4	Contamination by feldspar	The ratio of the L_x/T_x[b, c] values obtained from two identical regenerative doses measured with and without prior IR[e] stimulation (OSL[f] IR depletion ratio; Duller, 2003) was less than unity at 2σ
5	Saturated or non-intersecting grains	L_n/T_n[a, d] values equal to, or greater than, the Imax saturation limit of the dose-response curve at 2σ
6	Anomalous dose response curves	Those displaying a zero or negative response with increasing dose) or dose-response curves displaying very scattered L_x/T_x[b, c] values (i.e., those that could not be successfully fitted with the Monte Carlo procedure and, hence, did not yield finite equivalent dose values and uncertainty ranges)

[a] L_n: natural luminescence signal.
[b] L_x: luminescence signal associated with laboratory irradiation.
[c] T_x: test dose associated with a corresponding laboratory luminescence signal.
[d] T_n: test dose associated with the natural luminescence signal.
[e] IR: infrared (λ=1mm-700nm)
[f] OSL: optically stimulated luminescence

Dose Rate Calculations

Lithogenic radionuclide activity was measured on representative sediment sub-samples, removed from the exposed surfaces of the corer, following Alksnis *et al.* (1999). Concentrations of U, Th, K (Adamiec and Aitken 1998) were measured at Genalysis using inductively coupled plasma optical emission spectrometry (ICP-OES) and inductively coupled plasma mass spectrometry (ICP-MS). This was because the radioactivity of the sediments was below the detection limits of the high-resolution gamma ray spectrometers (HRGS) available at Adelaide University. The ionizing radiation rate (dose rate) resulting from the measured elemental concentrations was then calculated using standard dosimetric conversion factors (Guérin *et al.* 2015).

The cosmic radiation component of the dose rate was calculated according to the equations of Prescott and Hutton (1994). The altitude of the sampling site was assumed to be 21 m above sea level. Overburdening bulk density for each sample was calculated from the corrected LOI density values. The depth of the lake water above the site was assumed to be 1m based on present day field observations. The total depth of the sample, and therefore depth component in attributing cosmic radiation calculation, was the summation of the sample depth relative to the top of the corresponding core drives and the overlying water body.

Water content values derived from LOI measurements (saturated, compaction corrected and directly measured) were then incorporated into the total dose rate calculations. This is necessary because the long term water content of the sediment core has an attenuation effect on the dose absorbed by the grains selected for OSL dating.

Age calculation and Bayesian Modelling

The OSL age equation was used to obtain ages for samples using the respective equivalent dose and dose rate. Age-depth relations were modelled using OxCal (Version 4.2), an online Bayesian modelling software package (Bronk Ramsey 2008, Bronk Ramsey and Lee 2013). The depths associated with the plots were constrained between the water/sediment interface (0 cm and 1280 cm) with optical dating results input into the Bayesian model with their combined systematic and random uncertainty terms. The modelled ages were specified at 1 mm intervals to enable a continuous age-depth profile to be established. All modelled age ranges are reported as the 68.2% and 95.4% highest probability density function. Outliers were assessed at the 95% significance level using an add-on of the program produced by Bronk Ramsey (2009).

RESULTS

Core Log

The core sediments are dark brown/black organic rich peat with episodic changes in quartz abundance down core. Towards the base of both cores few and small lenses of quartz <1 cm were observed. At a depth of 1268 cm in WL15/2 the basal sand and lagoonal organic contact is preserved distinctly. The 1 m core drive containing the sediments below 1250 cm in the WL15/2 core also contained visible coarse grain quartz within the basal sediments.

ITRAX Data

The overlapping cores from Welsby Lagoon were scanned for elemental abundance through ITRAX to assess the core continuity. Although time constraints on the project

did not allow for corrections to breaks in the sediment nor smoothing of data, the ITRAX elemental data (Si, S, K Ca, Ti and Fe) showed agreement between cores WL15/1 and WL15/2 (Figure 5). ITRAX data highlights that there are increases in all elements near the bottom of the core at 9.0 m and further towards the base of the cores. The Si value increases rapidly in WL15/2 at the base more so than WL15/1 as intersected the basal sand layer.

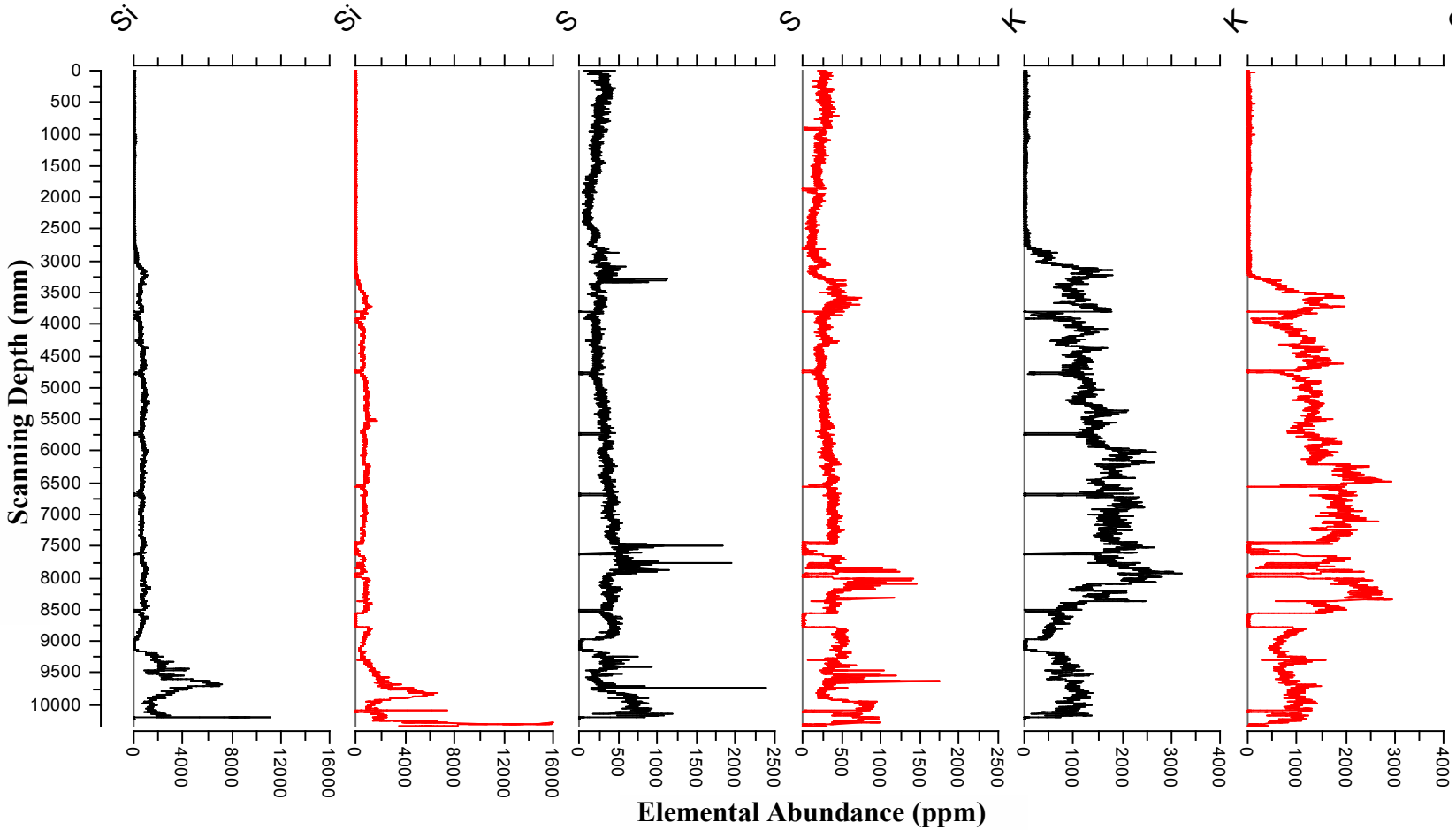

Figure 5: Elemental component abundances down core from scaning with the ITRAX core logger. Black line indicates core WL15/1, red line indicates core WL15/2.

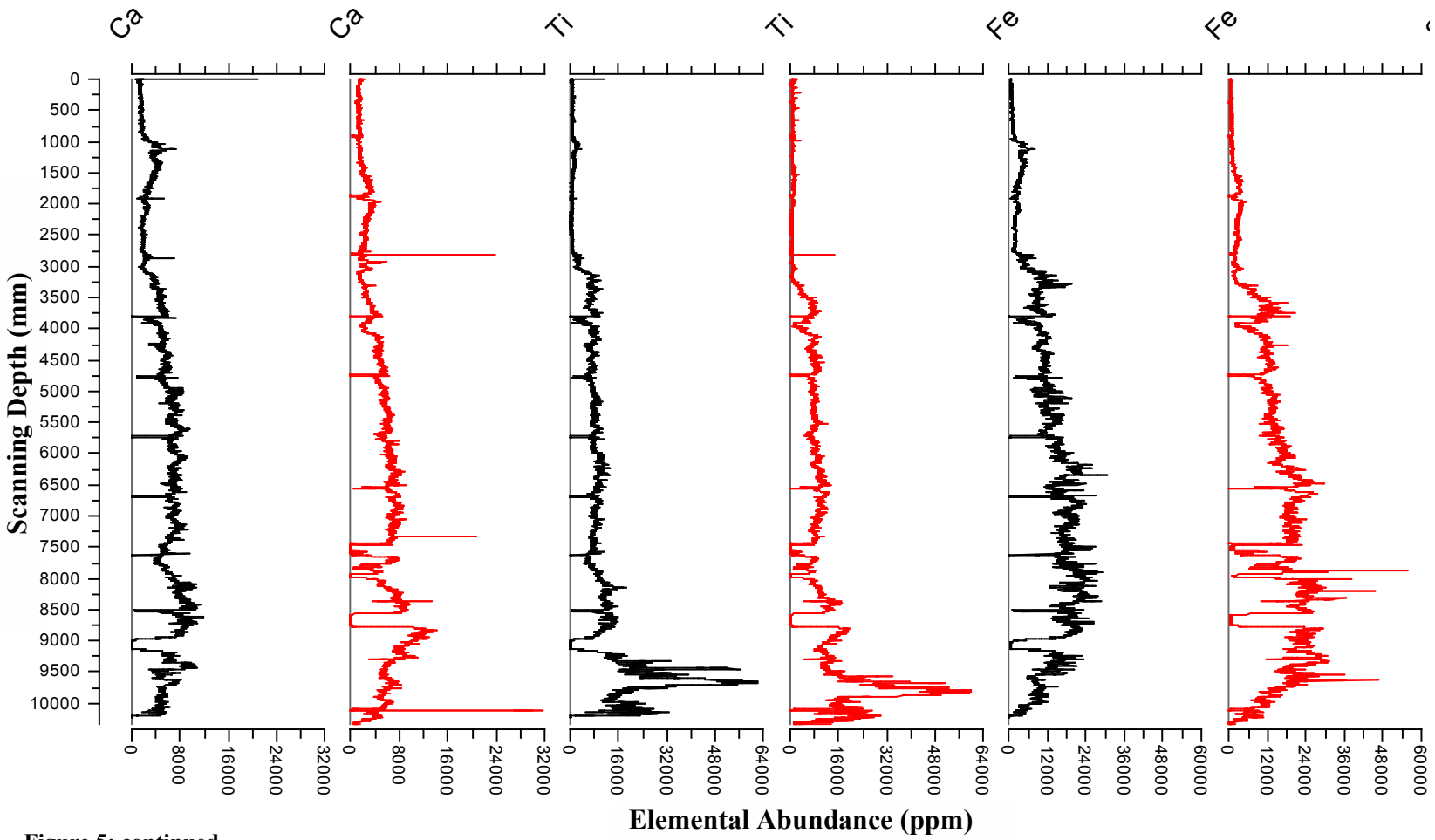

Figure 5: continued.

Water Content, Bulk Density and Grain Size

The Welsby Lagoon core WL15/2 is characterised by very high water content with average of 687% dry sediment weights (Figure 6). The water content within the top 600 cm of WL15/2 shows high variability with maximum and minimum values of 1413 and 485%. Meanwhile below this depth the water content maintains an average of 463% before decreasing rapidly at 1130 cm depth to a low of 26%.

The corrected bulk density of WL15/2 averages 1.03 g/cm^3 down the entire length of the core (Figure 6). The bulk density of the core does not reach above the density of water (1.0 g/cm^3) until a depth of 500 cm. Below 500 cm the bulk density values maintain an average of 1.34 g/cm^3 down to a depth of 1160 cm, before increasing significantly to peak at 1.62 g/cm^3 at 1270 cm depth.

Sampled depths shallower than 850 cm show an increased population (approximately 8–10% of total sample) of fine (<90 μm) particles in comparison to the basal layers (Figure 7). At depth 480 cm there is a distinct increase in fine particulates up to 36% in comparison to adjacent depths. Although the fine grained particle proportions are observed to fluctuate, the primary grain size through the core is >180 μm.

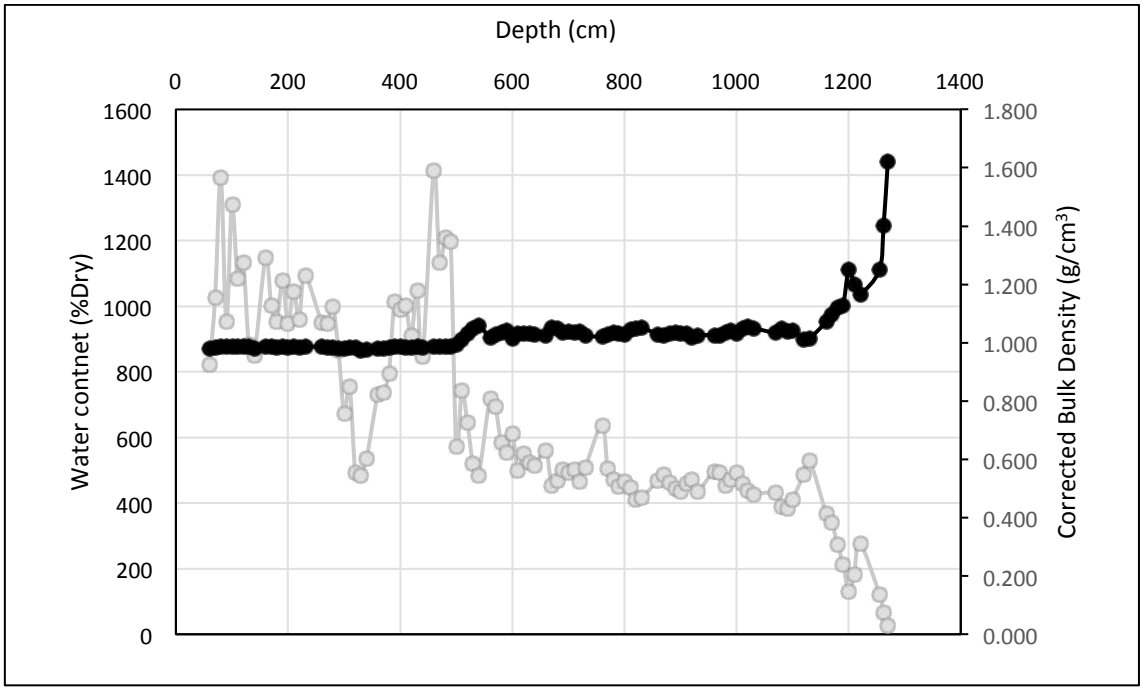

Figure 6: Measured water content (%Dry) calculated using a modified approach of Heiri *et al.* (2001) and corrected bulk density (g/cm^3) down core of WL15-2. Water content is in grey with sample points representing measured values with the grey line interpreting between. The black corrected bulk density line was calculated knowing the proportion of water, organic and inorganic matter from LOI in a 1 cm^3 sample assuming densities 1.00, 0.80 and 1.80 g/cm^3 respectively.

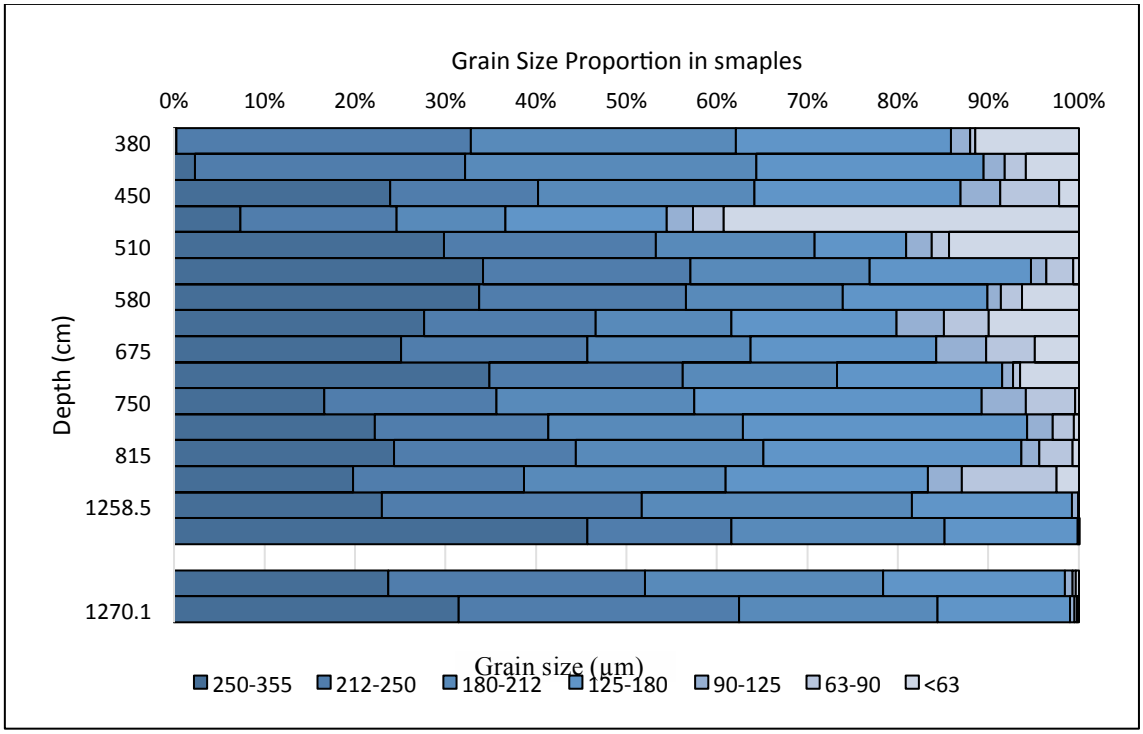

Figure 7: Grain size distribution down core WL15-2 derived from weighing sieved fractions for OSL dating. Fractions at a specific depth are shown as a percentage of the total weight of all fractions that represent that sample and determined by available sieves. The repeated 1258 cm and 1270 cm depths at the bottom of the graph are from core WL15-1.

Single-grain OSL Properties

Most of the Welsby Lagoon quartz samples have a <14% proportion of grains that meet the SAR selection criteria, which is at least partially due to the fact that most of the grains contained high proportions of considerably dim grains and anomalous dose-response properties (~70%) (Appendix B).

Equivalent Dose distributions

Sample decay-curves, dose response curves and equivalent dose distributions for sample WL2(7) are shown in (Figure 8). The brighter natural signals produced dose response curves with a larger linear component than exponential, this trend reverses as the signal decreases in brightness.

The natural signal of samples from Welsby Lagoon show individual D_e values which are predominantly normally distributed (Figure 9). The standard error for D_e values show proportionality between high and low D_e estimates in most cases. The samples also show that under the best conditions possible, over-dispersion values observed are predominantly around 20–30% and all overlap at 2σ, with the exception of WL2(9) which shows very high over-dispersion of 52.4%. The majority of the samples show symmetrical heterogeneous D_e distributions on the radial plot, except WL2(9) which shows more asymmetric scatter.

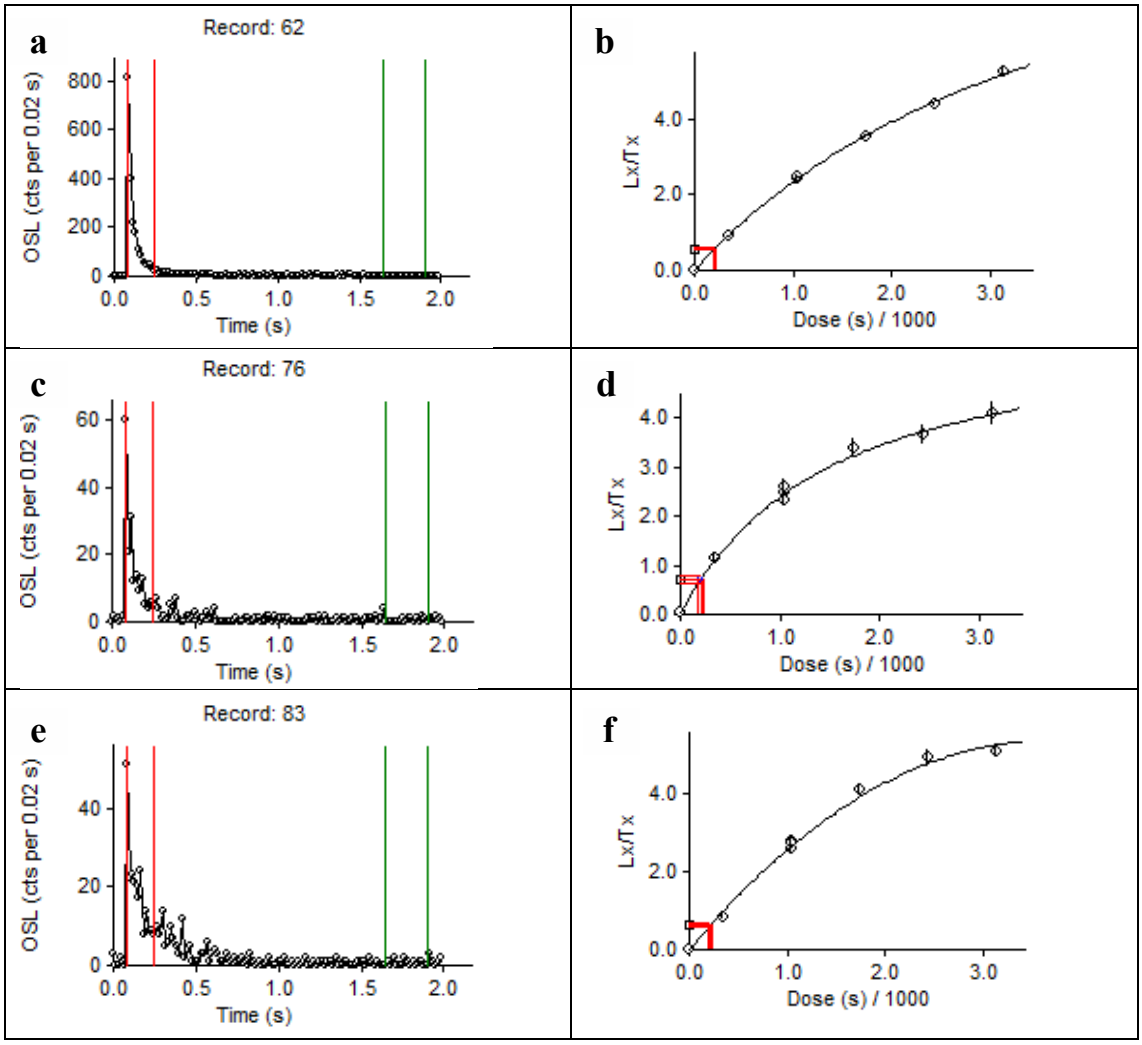

Figure 8: Natural signal (Ln) shine-down curves (a, c and e) for single-grain OSL samples from Welsby Lagoon (580 cm depth) with decreasing brightness. The vertical lines indicate the signal and background integration windows. Dose regeneration plots of sensitivity corrected OSL (Luminescence signal (Lx)/Test dose (Tx)) on the same aliquots are shown in b, d and f. The 2 sigma fit to the dose response curve is shown by intersecting lines.

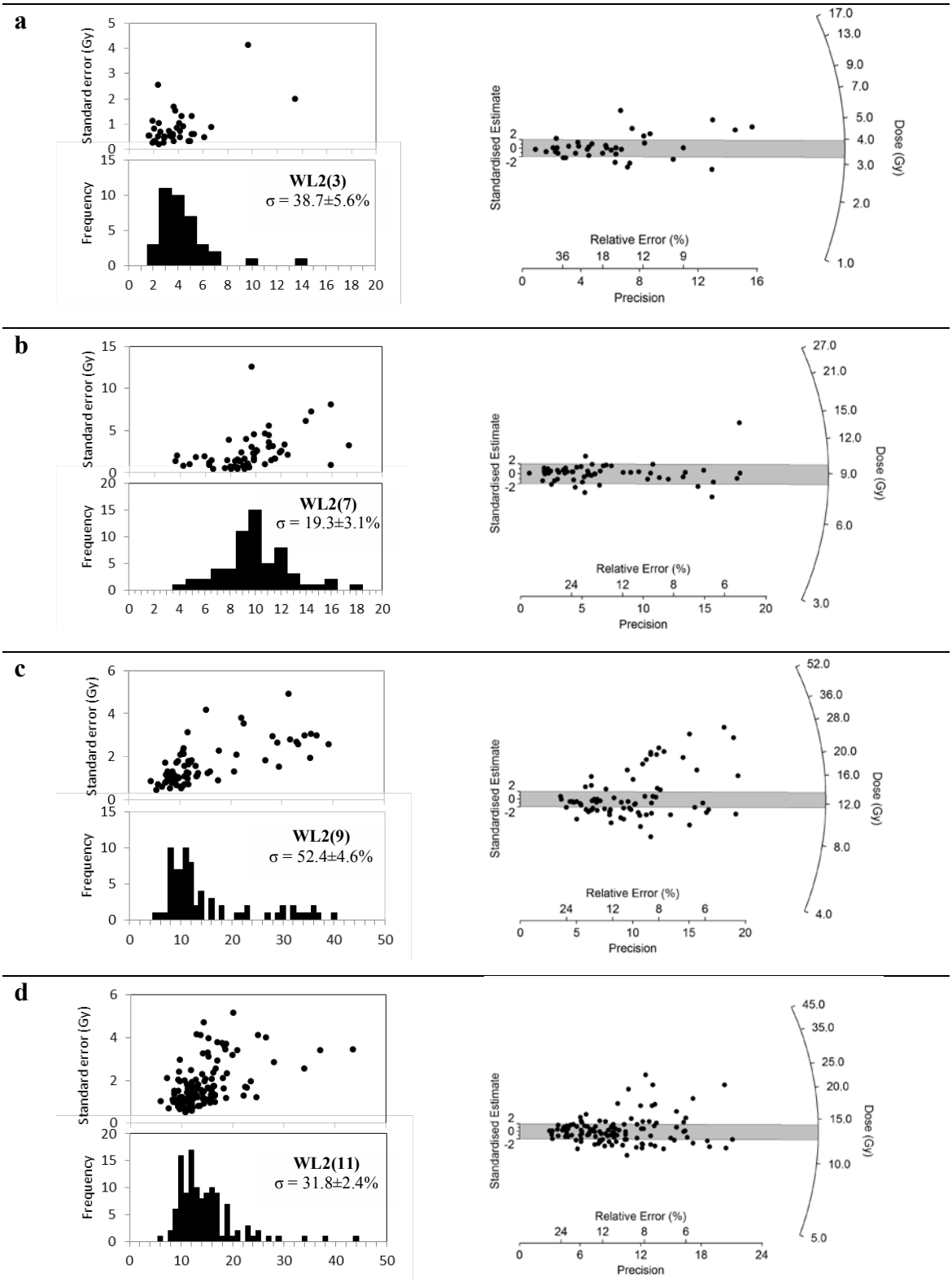

Figure 9: Natural single-grain D_e distributions of the samples from Welsby Lagoon, shown as frequency histograms and graphs of standard error versus D_e estimates, and radial plots. The shaded regions on the radial plots are centred on the burial dose estimates of the central age model (CAM) which provides a statistically suitable fit to each data set except sample WL2(9) with over-dispersion of 52.4±4.6. Individual D_e values that fall within the shaded region are consistent with the central dose estimate at ±2σ.

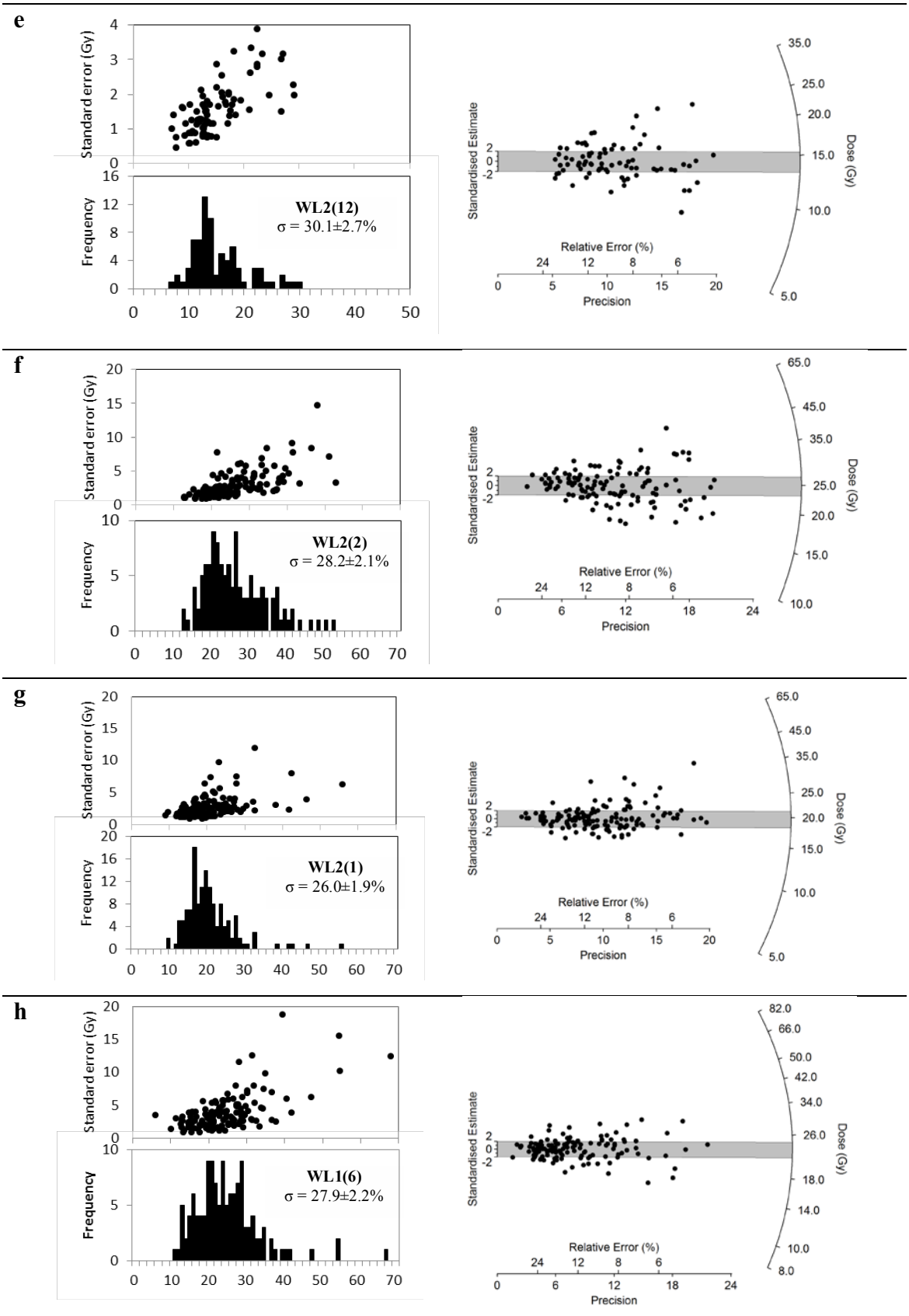

Figure 9: (*continued*)

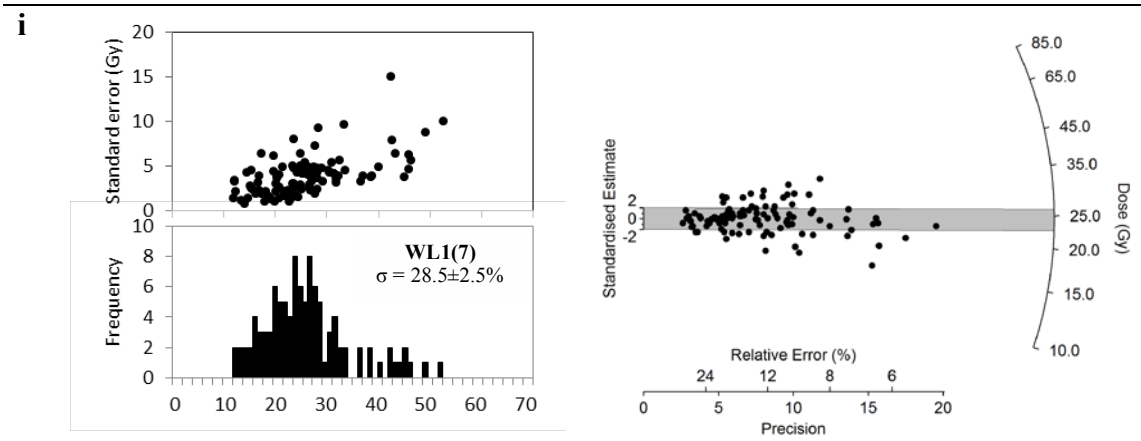

Figure 9: (*continued*)

Sample WL2(9) showed a positively skewed D_e distribution and a high (>50%) over dispersion value suggesting the central age model (CAM) was not a suitable fit. This suggested the grains had not been completely bleached prior to deposition or had experienced post depositional mixing. To investigate the likelihood of incomplete bleaching, WL2(9) was modelled using a minimum age model (MAM4) (Galbraith and Laslett 1993). Meanwhile the finite mixture model (FMM) was also used to investigate multiple grain populations related to mixing (Galbraith and Green 1990) (Figure 10). The MAM4 estimates a D_e value of 9.7 ± 0.7 Gy and focuses on the younger, "well bleached" grains in the population therefore reflecting the true signal accumulated 'in situ'. Meanwhile the FMM model distinguishes two components of D_e with values 9.80 ± 0.40 Gy and 28.9 ± 2.1 Gy. Although the results from the radial plots show either MAM4 or FMM are applicable for final D_e determination, MAM4 is chosen on the grounds that the D_e scatter likely originates from partially bleached grains, rather than post depositional mixing, because the driving mechanism of sediment transport is assumed to be very localised (short-distance) aeolian in origin. If this short distance transportation occurred under cloud cover or at night, there may have been limited

chance for complete bleaching of residual OSL signals prior to burial. Furthermore, the older grain population within the FMM is not represented anywhere else in the sedimentary core, suggesting mixing between layers is an unlikely explanation. Regardless, the ages obtained using the MAM4 and FMM correspond and are undistinguishable, meaning the final age is insensitive to the choice of age model in this circumstance.

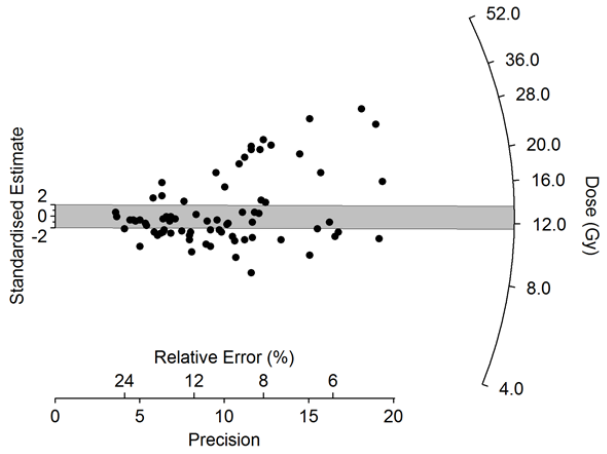	**Central Age Model (CAM)** Dose rate (Gy/ka):0.217 ± 0.026 D_e (Gy): 12.700 ± 0.796 Age (ka): 58.6 ± 7.9
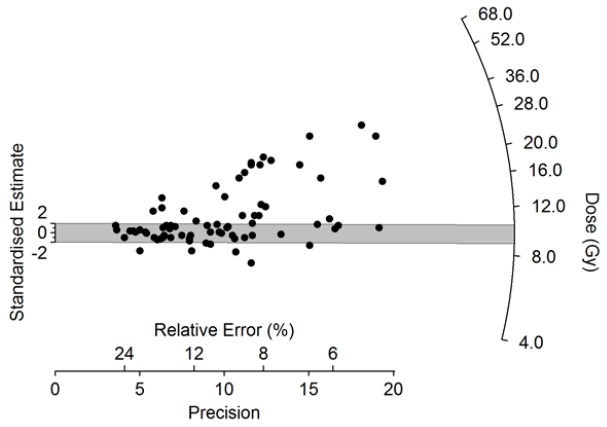	**Minimum Age Model (MAM4)** Dose rate (Gy/ka):0.217 ± 0.026 D_e (Gy): 9.678 ± 0.678 Age (ka): 44.6 ± 6.2
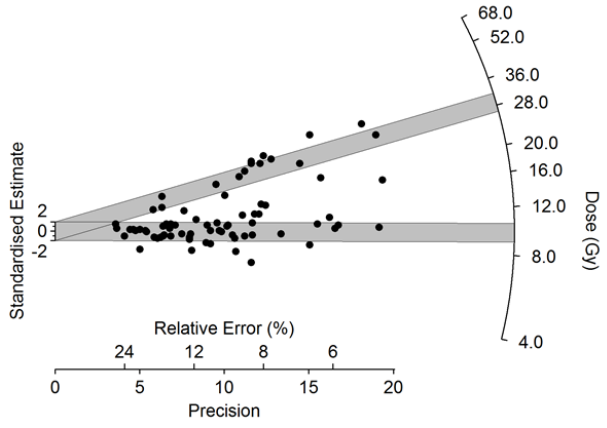	**Finite mixture Model (FMM)** Dose rate (Gy/ka):0.217 ± 0.026 D_e (Gy) Population 1: 9.796 ± 0.397 Population 2: 28.869 ± 2.135 Age (ka) Population 1: 45.2 ± 5.7 Population 2: 133.1 ± 18.7

Figure 10: Left: Radial plots of WL2(9) showing the D_e scatter in relation to the differing models (Top-Bottom: Central age model; minimum age model; Finite mixture model). The shaded regions on the radial plots are centred on the burial dose estimates of various models. Right: Values obtained when sample WL2(9), from a depth of 675 cm, is modelled with central age model (CAM), 4-component minimum age model (MAM4) and finite mixing model (FMM) using water content of 460 %Dry. Table includes values calibrated for sediment compaction and dewatering.

Dose Rate

The environmental dose rate in the Welsby Lagoon sediments was calibrated from the ICP-OES and ICP-MS data from Genalysis (Appendix C). Radionuclide contents are as low as 0.20±0.02 ppm uranium, 0.37±0.03 ppm thorium and 0.010±0.001% potassium (WL2(3) at depth 380 cm), leading to a dose rate of 0.132±0.022 Gy/ka (taking into account a measured water content of 963%Dry). Total environmental dose rates were relatively low with gamma and beta components contributing to >60% of the calculated dose rate (Table 6). Large water content in the upper part of the core resulted in lower dose rate values incomparison with the basal quartz rich sections. Notably, constraining the long term water content is crucial when calculating the dose rates due to its attenuation influences on ionising radiation. Due to the uncertainty in the long term water content of the site it was decided to test the impact of different water content histories. Three scenarios were tested: use of saturated water content values, directly measured (LOI) water content values and compaction corrected (calculated by assuming linear sedimentation and taking the water content at half the total sediment depth) models, and their effect on total dose rate.

Table 6: Water content and environmental dose rate components contributing to total dose rate of all OSL measured Welsby Lagoon samples. (a) water contents derived from saturated water content method, (b) water content values corrected for compaction from measured LOI samples, (c) water content directly measured form LOI sampling at given depth. For uranium, thorium and potassium abundance obtained from ICP-OES and ICP-MS refer to table in (Appendix C).

	Sample				Dose Rate (Gy/kg)				
	ID	Depth (cm)	Grain Size (μm)	Water (%)[a]	Gamma dose rate	Beta dose rate	Cosmic dose rate	Internal dose rate	Total dose rate
(a)	2.3	380	180–250	1053.3	0.043 ± 0.001	0.036 ± 0.015	0.013 ± 0.001	0.032 ± 0.011	0.125 ± 0.022
	2.7	580	212–250	1018.8	0.047 ± 0.001	0.037 ± 0.015	0.013 ± 0.001	0.032 ± 0.011	0.129 ± 0.022
	2.9	675	212–250	964.7	0.045 ± 0.001	0.038 ± 0.015	0.013 ± 0.001	0.032 ± 0.011	0.128 ± 0.021
	2.11	775	180–250	870.6	0.058 ± 0.001	0.049 ± 0.017	0.014 ± 0.001	0.032 ± 0.011	0.153 ± 0.024
	2.12	815	180–250	910.5	0.06 ± 0.001	0.053 ± 0.020	0.013 ± 0.001	0.032 ± 0.011	0.158 ± 0.026
	2.2	1258	212–250	209.1	0.113 ± 0.003	0.083 ± 0.006	0.054 ± 0.005	0.032 ± 0.011	0.282 ± 0.021
	1.7	1270	212–250	89.1	0.084 ± 0.004	0.059 ± 0.005	0.064 ± 0.006	0.032 ± 0.011	0.239 ± 0.019
(b)	2.3	380	180–250	963.2	0.047 ± 0.001	0.039 ± 0.015	0.014 ± 0.001	0.032 ± 0.011	0.132 ± 0.022
	2.7	580	212–250	894.3	0.053 ± 0.001	0.042 ± 0.015	0.014 ± 0.001	0.032 ± 0.011	0.142 ± 0.022
	2.9	675	212–250	861.6	0.05 ± 0.001	0.042 ± 0.015	0.015 ± 0.001	0.032 ± 0.011	0.138 ± 0.022
	2.11	775	180–250	827.2	0.061 ± 0.001	0.051 ± 0.017	0.015 ± 0.001	0.032 ± 0.011	0.159 ± 0.025
	2.12	815	180–250	813.4	0.067 ± 0.001	0.059 ± 0.02	0.015 ± 0.001	0.032 ± 0.011	0.172 ± 0.027
	2.2	1258	212–250	209.1	0.113 ± 0.003	0.083 ± 0.006	0.054 ± 0.005	0.032 ± 0.011	0.282 ± 0.021
	1.7	1270	212–250	89.1	0.084 ± 0.004	0.059 ± 0.005	0.064 ± 0.006	0.032 ± 0.011	0.239 ± 0.019

(c)

2.3	380	180–250	796.2	0.056	±	0.001	0.046	±	0.015	0.017	±	0.002	0.032	±	0.011	0.152	±	0.023
2.7	580	212–250	585.7	0.077	±	0.002	0.061	±	0.015	0.021	±	0.002	0.032	±	0.011	0.192	±	0.025
2.9	675	212–250	460.1	0.087	±	0.002	0.073	±	0.015	0.025	±	0.003	0.032	±	0.011	0.217	±	0.026
2.11	775	180–250	488.5	0.096	±	0.002	0.082	±	0.017	0.023	±	0.002	0.032	±	0.011	0.233	±	0.028
2.12	815	180–250	429.8	0.116	±	0.002	0.103	±	0.02	0.025	±	0.003	0.032	±	0.011	0.276	±	0.032
2.2	1258	212–250	80.9	0.139	±	0.003	0.103	±	0.007	0.068	±	0.007	0.032	±	0.011	0.342	±	0.022
1.7	1270	212–250	33.2	0.123	±	0.006	0.088	±	0.006	0.094	±	0.009	0.032	±	0.011	0.337	±	0.021

[a] percentage expressed as weight of dry sample.

OSL Chronologies

SINGLE-GRAIN

Water content values derived from saturated sediment measurements, compaction corrected water content and directly measured LOI (Table 7) differ significantly. For instance, sample WL1(7) at a depth of 1270 cm shows a 37% water content increase between measured and compaction corrected models, which leads to a change in age of ~30 ka.

Similarly, the ages for the base of the core derived from the OxCal models differ by 26 ka depending on long-term water content assumptions (Appendix D and E). Notably, only the water content compaction corrected (compaction) and directly measured water content (measured) age models (Figures 11–12) successfully plotted in OxCal. The measured saturated water content (saturated) age model was unable to plot in the program due to large errors associated with the ages and too few age constraints.

Both the measured and compaction age models project a chronologically linear tend down core. The suitability of each model's fit is determined by the individual agreement index (A_i), and the model agreement index (A_{model}) which quantify the correspondence between upper and lower sample age estimates for individual dated samples and for the model as a whole. The compaction age model showed an A_i and A_{model} value of 69.7% and 55.6%, while the measured age model showed values of 98.2% and 94.5% respectively. The OxCal add-on software highlighted outliers within the compaction age model, flagging three borderline outliers, samples WL2(7), WL2(11) and WL2(12). In contrast, there were no outliers identified in the measured age model. Assuming a 1σ confidence interval for the compaction (Figure 11)(Appendix E) and measured age

models (Figure 12) (Appendix D), the basal ages were modelled to be 99.7 ± 7.7 ka and 76.9 ± 3.9 ka respectively.

Table 7: Accepted single-grain summary table for the Welsby Lagoon samples. (a) saturated samples (b) compaction corrected samples with basal saturated (c) LOI measured samples. Corresponding ages were used to model using OxCal.

	Sample WL	Depth (cm)	Grain Size (μm)	Accepted grains/ measured	Water content (%)[a]	Over-dispersion (%)	Dose rate (Gy/ka)	D_e (Gy)	Age (ka)
(a)	2(03)	380	180–250	40/500	1053	38.7 ± 5.6	0.125 ± 0.022	3.605 ± 0.256	29.0 ± 5.4
	2(07)	580	212–250	61/900	1018	19.3 ± 3.1	0.129 ± 0.022	9.037 ± 0.314	69.9 ± 12.1
	2(09)	675	212–250	74/800	964	20.0 ± 0.0	0.128 ± 0.021	9.678 ± 0.678	75.7 ± 13.7
	2(11)	775	180–250	120/800	870	31.8 ± 2.4	0.153 ± 0.024	13.429 ± 0.422	88.0 ± 14.5
	2(12)	815	180–250	79/800	910	30.1 ± 2.7	0.158 ± 0.026	14.262 ± 0.514	90.1 ± 15.4
	2(02)	1258	212–250	120/900	209	28.2 ± 2.1	0.282 ± 0.021	24.993 ± 0.696	88.7 ± 7.4
	1(07)	1270	212–250	106/600	89	28.5 ± 2.5	0.239 ± 0.019	24.483 ± 0.769	102.4 ± 8.9
(b)	2(03)	380	180–250	40/500	963	38.7 ± 5.6	0.132 ± 0.022	3.605 ± 0.256	27.2 ± 4.9
	2(07)	580	212–250	61/900	894	19.3 ± 3.1	0.142 ± 0.022	9.037 ± 0.314	63.8 ± 10.4
	2(09)	675	212–250	74/800	861	20.0 ± 0.0	0.138 ± 0.022	9.678 ± 0.678	69.9 ± 12.1
	2(11)	775	180–250	120/800	827	31.8 ± 2.4	0.159 ± 0.025	13.429 ± 0.422	84.7 ± 13.6
	2(12)	815	180–250	79/800	813	30.1 ± 2.7	0.172 ± 0.027	14.262 ± 0.514	83.1 ± 13.4
	2(02)	1258	212–250	120/900	209	28.2 ± 2.1	0.282 ± 0.021	24.993 ± 0.696	88.7 ± 7.4
	1(07)	1270	212–250	106/600	89	28.5 ± 2.5	0.239 ± 0.019	24.483 ± 0.769	102.4 ± 9.1

(c)

2(03)	380	180–250	40/500	796	38.7 ± 5.6	0.152	±	0.023	3.605 ± 0.256	23.8	± 4.1
2(07)	580	212–250	61/900	585	19.3 ± 3.1	0.192	±	0.025	9.037 ± 0.314	47.1	± 6.4
2(09)	675	212–250	74/800	460	20.0 ± 0.0	0.217	±	0.026	9.678 ± 0.678	44.6	± 6.2
2(11)	775	180–250	120/800	488	31.8 ± 2.4	0.233	±	0.028	13.429 ± 0.422	57.6	± 7.3
2(12)	815	180–250	79/800	429	30.1 ± 2.7	0.276	±	0.032	14.262 ± 0.514	51.6	± 6.3
2(02)	1258	212–250	120/900	80	28.2 ± 2.1	0.342	±	0.022	24.993 ± 0.696	72.6	± 5.4
1(07)	1270	212–250	106/600	33	28.5 ± 2.5	0.337	±	0.021	24.483 ± 0.769	73.1	± 5.2

[a] percentage expressed as weight of dry sample.

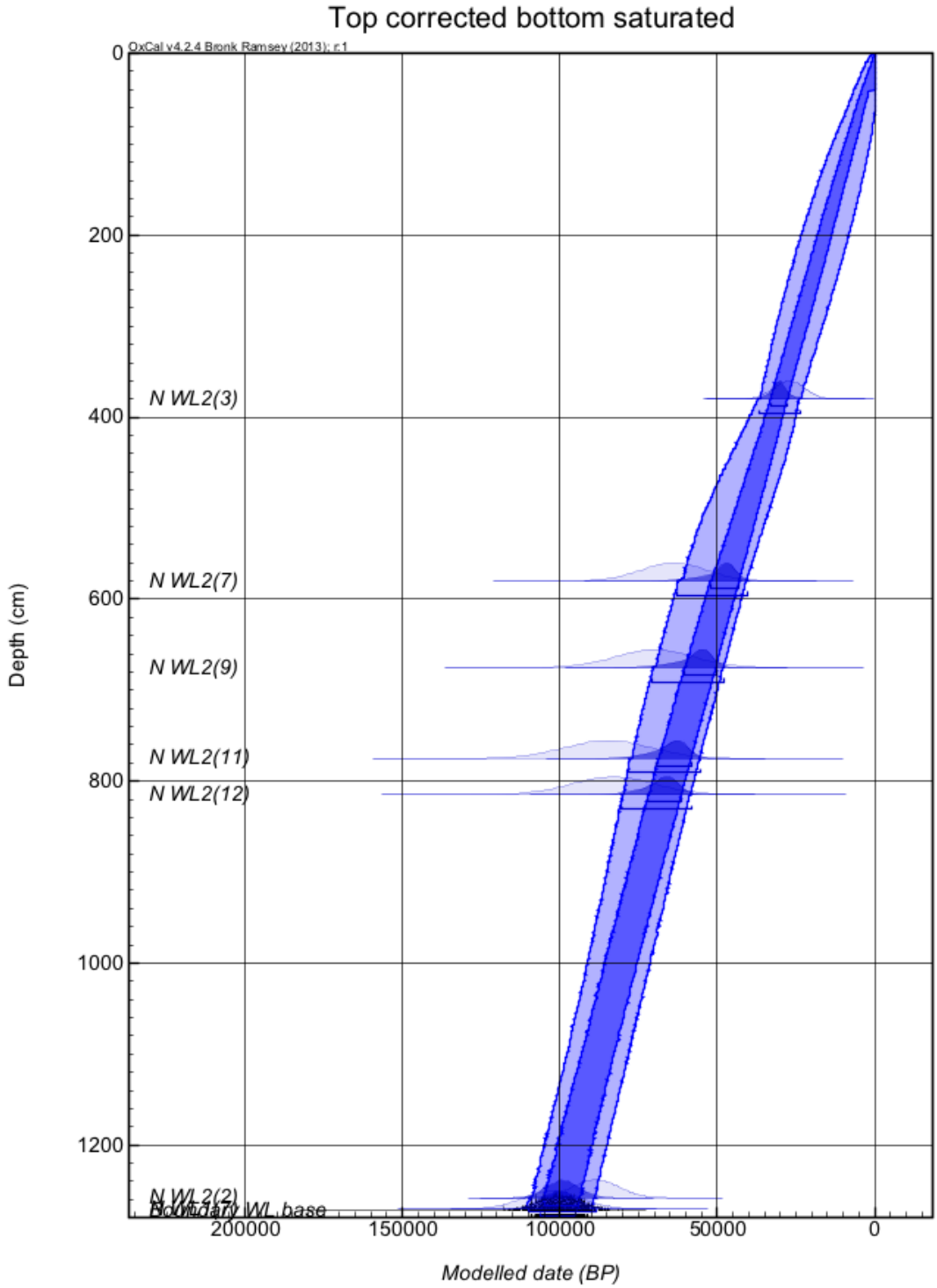

Figure 11: Compaction corrected Bayesian age model with saturated basal sands, obtained through OxCAL Version 4.2, using six OSL ages from samples in WL15/2 and 1 from WL15/1, projecting ages from 0cm (sediment/water interface) to 1300cm below surface. Dark blue represents 1σ interval, medium blue represents 2σ modelled interval. The prior age distributions for the dating samples (likelihoods) are shown in light blue. The modelled posterior distributions for the dating sample and stratigraphic unit boundaries are shown in dark blue.

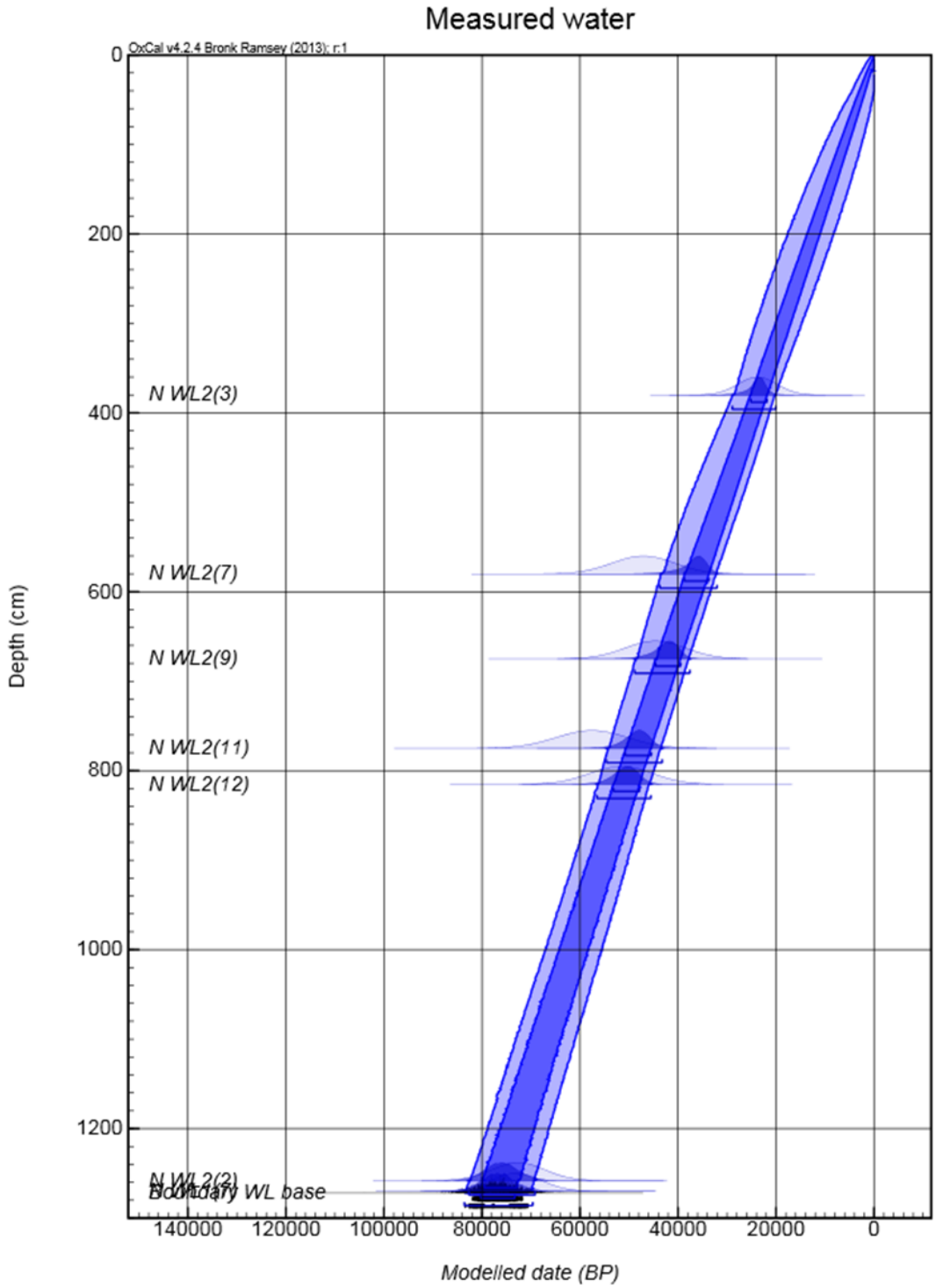

Figure 12: Bayesian age record derived using measured moisture content through LOI (not corrected for post-depositional compaction) model, obtained through OxCAL Version 4.2, using six OSL ages from samples in WL15/2 and 1 from WL15/1, projecting ages from 0cm (sediment/water interface) to 1300cm below surface. Dark blue represents 1σ interval, medium blue represents 2σ interval. The prior age distributions for the dating samples (likelihoods) are shown in light blue. The modelled posterior distributions for the dating sample and stratigraphic unit boundaries are shown in dark blue.

MULTI-GRAIN VS SINGLE-GRAIN

'Synthetic' multi-grain aliquot D_e values (and ages), were created by surveying the included D_e values of the 100 grain compounded on each SG disk to assess the feasibility of routine MG-OSL dating at this site. The respective multi-grain D_e distributions primarily show a decrease in over-dispersion by ~10%, excluding samples near the upper section of the core which increase by more than 50% (Table 8). The estimated D_e values of the multi grain analysis show an average increase of 3.15 Gy. Furthermore, the increased D_e values of the multi-grain and their respective errors with respect to single grain analysis translate to large age overestimations. Comparative ages between the multi-grain and single-grain methods show an overestimation by an average of 31% with respect to the single-grain method. Notably, the multi-grain method also shows age uncertainties that are significantly larger than at the single-grain scale of analysis with a maximum difference of 155 ka.

Table 8 Changes in over-dispersion, equivalent dose and age estimation between multi-grain and single grain OSL analysis. (a) water contents derived from saturated water content method, (b) water content values corrected for compaction from measured LOI samples, (c) water content directly measured. Negative values correspond to higher single-grain values with respect to their corresponding multigrain values (Appendix F).

	Sample	Depth (cm)	Water (%)[a]	Δ^b Over-dispersion (%)			Δ^b D_e (Gy)			Δ^b Age		
(a)	2(03)	380	1053	50.5	±	-5.235	1.237	±	2.24	9925	±	15710
	2(07)	580	1019	22	±	-2.969	0.62	±	1.472	4765	±	6629
	2(09)[a]	675	964	2.6	±	0.066	8.516	±	1.007	66454	±	13413
	2(11)	775	870	-15.8	±	-2.357	1.479	±	0.488	9594	±	2325
	2(12)	815	910	-9.3	±	-2.613	-0.48	±	1.16	-3095	±	2566
	2(02)	1258	209	-13.1	±	-2.056	1.603	±	0.954	39724	±	155172
	1(07)	1270	89	-16.9	±	-2.462	9.091	±	1.005	37591	±	4652
(b)	2(03)	380	963	50.5	±	-5.235	1.237	±	2.24	9329	±	14872
	2(07)	580	894	22	±	-2.969	0.62	±	1.472	4345	±	6235
	2(09)a	675	861	2.6	±	0.066	8.516	±	1.007	61462	±	11955
	2(11)	775	827	-15.8	±	-2.357	1.479	±	0.488	9253	±	2225
	2(12)	815	813	-9.3	±	-2.613	-0.48	±	1.16	-2851	±	2523
	2(02)	1258	209	-13.1	±	-2.056	1.603	±	0.954	39724	±	155172
	1(07)	1270	89	-16.9	±	-2.462	9.091	±	1.005	37591	±	4652
(c)	2(03)	380	796	50.5	±	-5.235	1.237	±	2.24	8156	±	13184
	2(07)	580	585	22	±	-2.969	0.62	±	1.472	3203	±	5019
	2(09)a	675	460	2.6	±	0.066	8.516	±	1.007	39315	±	6501
	2(11)	775	488	-15.8	±	-2.357	1.479	±	0.488	6333	±	1452
	2(12)	815	429	-9.3	±	-2.613	-0.48	±	1.16	-1771	±	2078
	2(02)	1258	80	-13.1	±	-2.056	1.603	±	0.954	5031	±	92746
	1(07)	1270	33	-16.9	±	-2.462	9.091	±	1.005	26172	±	3066

[a] percentage expressed as weight of dry sample.
[b] Δ = ((multi-grain) – (single grain))

DISCUSSION

SEDIMENTOLOGY

Water Content

There are two possible hypothesis for establishing the past long term water content in Welsby Lagoon. The first is assuming that the lagoonal sediment water content, as directly measured with LOI, is representative of the past water content. This scenario assumes that capillary forces between the fine organic sediments were strong enough to retain the original water content during coring and transport (Corbett *et al.* 1992). While this assumption seems reasonable, the same cannot be said for the lower sandy sections of the cores. Here, the larger grains are less capable at retaining water, explaining the lower water content (33% dry) at the base.

An alternate hypothesis for the water content is that the recorded long term water content of the samples had reduced over time. This could have come about because of compaction squeezing of water from the lower sediments as pressure increased from progressive build-up of overlying sediments and reduced pore space. Although it is difficult to completely asses compaction effects within the scope of this project, it was assumed to have exerted at least some effect down the length of the core. The compactibility of the organics in the lacustrine sediments is likely higher than the transitional or sandy basal zone due to the greater abundance of resistive quartz in the latter. This means that the long term water content would have been preserved to a better extent in the less compacted base of the core, compared to the more compacted top of the core.

Bulk Density

Assuming no compaction, the bulk density of lagoonal sediments above 500 cm down core were noted to be an average of 0.986g/cm^3. This is because the majority of that sediment consisted of less dense organic peat (~0.801 g/cm^3) rather than water or inorganic material. The increase in bulk density (average 1.032 g/cm^3) between 500 – 1130 cm results from a higher inorganic to organic ratio, largely because of an increase in sand/dust transport into the system. Finally, below this transitional region organic content reduces drastically, leading to a bulk density which trends towards pure sand (~1.800 g/cm^3) which corresponds to the formation of the lagoon within the sands of North Stradbroke Island when sand and water was in close proximity. Notably if we assume compaction to have been experienced, then the increasing density results from decreasing pore space as well as changing sedimentology.

Dust/Grain Sizes

The source of quartz grains in Welsby Lagoon sediments has been hypothesised to originate from the surrounding dunes largely as aeolian forcing from the south-east is prevalent on North Stradbroke Island (Ward 1978, Petherick *et al.* 2011, Lamy *et al.* 2014).This study showed that the majority of samples had a significant population (~70%) consisting of grains with diameter >180 μm. This supports the hypothesis of localized sourcing from dune sands which were found to have a modal grain size between 180–250 μm (Thompson and Bowman 1984, Tejan-Kella *et al.* 1990, Thompson 1992). Notably, this study also showed that there was variability in the finer grain sizes <90 μm in particular. Although the resolution of this study did not allow precise analysis of this smaller fraction, it does suggest that there is variability in larger distance dust input to the site. This variability is emphasised particularly at 480 cm

where <63 μm grains increases to represent ~40% of the grain population. Assuming the measured water content age-depth model is correct, the flux in finer grains in sample at 480 cm were modelled at ages 31.8–27.7 ka (1σ confidence interval) and 36.5–26.0 ka (2σ confidence interval; Refer Appendix D) which is broadly consistent with the timing of increased dust deposition on North Stradbroke Island (Petherick *et al.* 2011), suggesting increased wind strength during this period. Elemental Composition (ITRAX) Although the ITRAX data was not able to be smoothed due to time constraints, variations in the elemental data does show a series of relationships pertaining to a flux in terrestrially sourced dust. The silicate abundance highlights the change in inorganic material and therefore assumed to be sand sourced from the surrounding dunes. Notably the increase in Fe and Ti support the hypothesis of an existing terrestrial dust record along with low Fe/K, and high Fe/Ca ratios as explored in previous climate dust studies by Adegbie *et al.* (2003), Hesse (1994). Unfortunately, due to the lack of smoothing in the elemental signals it is difficult to identify substantial changes which may be attributed to climatic variability. However, it should be noted that the ITRAX data does suggest that the sediment record is continuous.

DOSE RATE

Constraining the long term water content, as stated earlier, proved difficult in this core. Due the proportionate relationship between water content and the dose rate, not being able to completely constrain the water transfers to uncertainty in the dose rate. This is because water has an attenuating effect on the ionizing radiation incident on the grain. Notably at the single grain scale, individual grains may exist within the sediment matrix adjacent to differing ratios of matter and water. In this project it was assumed that each individual grain of a sample experienced contact with the same water ratio.

The K, U and Th concentrations, obtained through ICP-MC and ICP-OES (Appendix C), show and increasing trend down core until reaching the lower sandy sections. The increasing trend is likely due to the accumulation of organic material rather than subsurface sourcing from the water table. This is because the island predominantly consists of silicates which only host trace amounts of these elements. Notably the latter also explains the decrease observed in the lower sections of the core. At these deeper sections the ratio of sand to organics increases and therefore there is a reduction in the abundance of K, U or Th. This study also assumed that the material sent for analysis was representative and that there was no close proximity large heterogeneities in the lagoon such as large organics or rocks which would have resulted in underestimations of the dose rate (Olley *et al.* 1999).

OSL CHRONOLOGIES

Multi-grain vs Single-grain

The ages of the multi-grain OSL samples at Welsby Lagoon, were disproportionately large compared to their single-grain counterparts. The multi-grain results were systematically higher by 4000 to 9000 years for the 7 samples. This is attributed to the 'masking' effect that the multigrain method produces (Arnold and Roberts 2009). The masking effect of the multi-grain analysis occurs from averaging all of a sample grain population and the inclusion of otherwise potentially problematic grains that are otherwise rejected (unsuitable) at the single-grain level..

With fewer D_e measurements in the multi-grain datasets, the models (CAM, MAM4) have true grain populations that are not well defined and therefore the associated D_e uncertainties are higher. By comparison, this the single grain measurements are mostly

in excess of 100 D_e values per sample. To produce a representative spread of D_e values comparable to the single-grain using multi-grain method approximately 100,000 grains are required at 100 grains per disk. Notably this quartz grain yield would surpass that removed from most of the samples from Welsby Lagoon, thereby requiring a decrease in sample resolution. Taking into account quartz availability, the age overestimations, and bleaching of WL2(9) (as seen in section4.5.), it is recommended that single-grain analysis is undertaken for future studies at Welsby Lagoon.

Single-grain OxCal Models

This study provided two Bayesian age-depth models through OxCal online software based on water contents from as measured and compaction correction scenarios (it is assumed that the saturated water content model had age uncertainties which produced adequate convergence in OxCal). Two OSL samples from WL15/1 and WL15/2, at depths of 1258 cm and 1270 cm, respectively, were omitted from the model (WL1(6) and WL2(1)) because of the uncertainty in the long term water contents. The σA_{model} and $A_{overall}$ values for the compaction corrected and measured Welsby Lagoon sequence were 69.7% and 55.6%, and 98.2% and 94.5%, respectively, which are considered viable on structural grounds.

The small σA_{model} and $A_{overall}$ values obtained in the compaction corrected model indicate that one or more OSL ages represent a statistical outlier. Using the add-on package OxCal identifies, these outliers to be samples WL2(11) and WL2(7), along with potentially sample WL2(12). Conversely, the higher σA_{model} and $A_{overall}$ values obtained for the as measured water content model reveal no distinct outliers in the data and therefore suggests that it is the better statistical model for the chronological dataset.

Accepting the measured water content model reveals an age of 76.9 ± 3.9 ka or 77.0 ± 6.5 ka at the 1σ and 2σ confidence interval for the basal sediments within the lagoon. This suggests formation of Welsby Lagoon during the onset of MIS 4 (71.0 ka).

CONCLUSIONS

This project has demonstrated that Welsby Lagoon, North Stradbroke Island is indeed datable beyond the radiocarbon barrier using OSL dating. The abundance of well bleached sand grain populations and capability of modelling the D_e values with CAM, indicates that a strong OSL chronological control can be derived from to the lagoonal sediments. However, due to the associated overestimation of ages that coincides with traditional OSL multi-grain analysis, together with evidence of partial bleaching and low quartz yield down core, it is recommended that single-grain dating be utilised for further studies in Welsby Lagoon.

This study has shown that it is possible to construct an age-depth model for Welsby Lagoon using OSL dating. However, the long term water content for the basal sands remains uncertain due to the suspected variability in capillary forces retaining water during extraction and storage, as well as undefined long-term sediment compaction effects. Therefore, for modelling purposes, further age constraints at the top of the core using radiocarbon dating and further OSL dating in-between 815 cm and 1258 cm are required before a definitive age model can be determined for the formation of the lagoon.

The sediments in Welsby Lagoon show evidence of containing a continuous record, occurring over at least the last 76.9 ± 6.5 ka and possibly as long as the last 102.4 ± 9.0 ka. This is highlighted in the ITRAX and OSL chronologies which do not show any signs of truncations or stepped age-depth profiles that would suggest the presence of

unconformities in the sediment. This interpretation supports the theory that the lagoon was able to continuously source adequate water from the perched water table preventing its drying in the past, and may explain the linear sedimentation evident in the developed age models. Furthermore, the fluctuations in grain size suggest periods of climatic variability, with an increase in fine grains <90 μm at 480 cm dated at 36.5 ± 26.1 ka (2σ confidence interval) corresponding to evidence of enhanced dust deposition on the island (Petherick et al 2008). However, at this stage to establish the ecosystems change with respect to climate, future studies at Welsby Lagoon should focus on charcoal, stable isotope, further grain size characterisation, rare earth element and pollen analysis for comparison with Greenland records to identify lead and lag events between Northern and southern hemispheres (Barbante *et al.* 2006, De Deckker *et al.* 2012).

Given the ability to place direct chronological constraints on the record, as well the preservation of a continuous record through at least 76.9 ± 6.5 ka, this project has demonstrated that Welsby Lagoon has the potential to provide a valuable record and make a significant contribution to our understanding of Australian palaeoclimates.

ACKNOWLEDGMENTS

I thank my supervisor Lee Arnold for his guidance in carrying out the project along with co-supervisors Nigel Spooner, John Tibby and Cameron Barr. I thank the Prescott Environmental Luminescence Laboratory at The University of Adelaide for the use of its space and equipment, along with laboratory technician Priya Whee. We thank Glenn McGregor and John Marshall from the Queensland Department of Science, Information Technology, Innovation and the Arts for assistance in collecting the Welsby Lagoon samples in this study. Further thanks is extended to Katie Howard and Rosalind King for their assistance throughout the year.

REFERENCES

ADAMIEC G. & AITKEN M. J. 1998 Dose-rate conversion factors: update, *Ancient tL,* vol. 16, no. 2, pp. 37-50.
ADEGBIE A., SCHNEIDER R., RÖHL U. & WEFER G. 2003 Glacial millennial-scale fluctuations in central African precipitation recorded in terrigenous sediment supply and freshwater signals offshore Cameroon, *Palaeogeography, Palaeoclimatology, Palaeoecology,* vol. 197, no. 3, pp. 323-333.
AITKEN M. J. 1998 An introduction to optical dating. Oxford University Press, Oxford.
ALKSNIS H., HUNT D. & WALLBRINK P. 1999 Radionuclides in the environment training manual, *CSIRO Land and Water Environmental Hydrology Group Technical Report,* vol. 30, no. 8, p. 1999.
ARNOLD L. J. & ROBERTS R. G. 2009 Stochastic modelling of multi-grain equivalent dose (De) distributions: Implications for OSL dating of sediment mixtures, *Quaternary Geochronology,* vol. 4, no. 3, pp. 204-230.
ATHY L. F. 1930 Density, porosity, and compaction of sedimentary rocks, *AAPG Bulletin,* vol. 14, no. 1, pp. 1-24.
BAKER V. R., PICKUP G. & POLACH H. A. 1985 Radiocarbon dating of flood events, Katherine Gorge, Northern Territory, Australia, *Geology,* vol. 13, no. 5, pp. 344-347.
BARBANTE C., BARNOLA J. M., BECAGLI S., BEER J., BIGLER M., BOUTRON C., BLUNIER T., CASTELLANO E., CATTANI O., CHAPPELLAZ J., DAHL-JENSEN D., DEBRET M., DELMONTE B., DICK D., FALOURD S., FARIA S., FEDERER U., FISCHER H., FREITAG J., FRENZEL A., FRITZSCHE D., FUNDEL F., GABRIELLI P., GASPARI V., GERSONDE R., GRAF W., GRIGORIEV D., HAMANN I., HANSSON M., HOFFMANN G., HUTTERLI M. A., HUYBRECHTS P., ISAKSSON E., JOHNSEN S., JOUZEL J., KACZMARSKA M., KARLIN T., KAUFMANN P., KIPFSTUHL S., KOHNO M., LAMBERT F., LAMBRECHT A., LAMBRECHT A., LANDAIS A., LAWER G., LEUENBERGER M., LITTOT G., LOULERGUE L., LÜTHI D., MAGGI V., MARINO F., MASSON-DELMOTTE V., MEYER H., MILLER H., MULVANEY R., NARCISI B., OERLEMANS J., OERTER H., PARRENIN F., PETIT J. R., RAISBECK G., RAYNAUD D., RÖTHLISBERGER R., RUTH U., RYBAK O., SEVERI M., SCHMITT J., SCHWANDER J., SIEGENTHALER U., SIGGAARD-ANDERSEN M. L., SPAHNI R., STEFFENSEN J. P., STENNI B., STOCKER T. F., TISON J. L., TRAVERSI R., UDISTI R., VALERO-DELGADO F., VAN DEN BROEKE M. R., VAN DE WAL R. S. W., WAGENBACH D., WEGNER A., WEILER K., WILHELMS F., WINTHER J. G. & WOLFF E. 2006 One-to-one coupling of glacial climate variability in Greenland and Antarctica, *Nature,* vol. 444, no. 7116, pp. 195-198.
BJÖRCK S. & WOHLFARTH B. 2001 14C chronostratigraphic techniques in paleolimnology. Tracking environmental change using lake sediments. pp. 205-245. Springer.
BLAAUW M., VAN GEEL B., MAUQUOY D. & VAN DER PLICHT J. 2004 Carbon-14 wiggle-match dating of peat deposits: advantages and limitations, *Journal of Quaternary Science,* vol. 19, no. 2, pp. 177-181.
BØTTER-JENSEN L., BULUR E., DULLER G. A. T. & MURRAY A. S. 2000 Advances in luminescence instrument systems, *Radiation Measurements,* vol. 32, pp. 523-528.
BOWLER J., QI H., KEZAO C., HEAD M. & BAOYIN Y. 1986 Radiocarbon dating of playa-lake hydrologic changes: examples from northwestern China and central Australia, *Palaeogeography, Palaeoclimatology, Palaeoecology,* vol. 54, no. 1, pp. 241-260.
BROECKER W., BOND G., KLAS M., CLARK E. & MCMANUS J. 1992 Origin of the northern Atlantic's Heinrich events, *Climate Dynamics,* vol. 6, no. 3-4, pp. 265-273.
BRONK RAMSEY C. 2008 Deposition models for chronological records, *Quaternary Science Reviews,* vol. 27, no. 1-2, pp. 42-60.
BRONK RAMSEY C. 2009 Dealing with outliers and offsets in radiocarbon dating, *Radiocarbon,* vol. 51, no. 3, pp. 1023-1045.
BRONK RAMSEY C. & LEE S. 2013 Recent and Planned Developments of the Program OxCal, *Radiocarbon,* vol. 55, no. 2-3, pp. 720-730.
BROOKE B., PREDA M., LEE R., COX M., OLLEY J., PIETSCH T. & PRICE D. 2008 Development, composition and age of indurated sand layers in the Late Quaternary coastal deposits of northern Moreton Bay, Queensland, *Australian Journal of Earth Sciences,* vol. 55, no. 2, pp. 141-157.
CHIANG J. C. H. & FRIEDMAN A. R. 2012 Extratropical Cooling, Interhemispheric Thermal Gradients, and Tropical Climate Change, *Annual Review of Earth and Planetary Sciences,* vol. 40, no. 1, pp. 383-412.
CLIFFORD H. T. & SPECHT R. L. 1979 The Vegetation of North Sradbroke Island. University of Queensland, St. Lucia, Australia.
COHEN T. J., JANSEN J. D., GLIGANIC L. A., LARSEN J. R., NANSON G. C., MAY J. H., JONES B. G. & PRICE D. M. 2015 Hydrological transformation coincided with megafaunal extinction in central Australia, *Geology,* vol. 43, no. 3, pp. 195-198.

COLLS K. & WHITAKER R. 1990 The Australian Weather Book. Associates Publishing Pty Ltd, Sydney, Australia.
CORBETT P., RINGROSE P., JENSEN J. & SORBIE K. 1992 Laminated clastic reservoirs: the interplay of capillary pressure and sedimentary architecture. SPE Annual Technical Conference and Exhibition. Society of Petroleum Engineers.
DANSGAARD W., JOHNSEN S., CLAUSEN H., DAHL-JENSEN D., GUNDESTRUP N., HAMMER C., HVIDBERG C., STEFFENSEN J., SVEINBJÖRNSDOTTIR A. & JOUZEL J. 1993 Evidence for general instability of past climate from a 250-kyr ice-core record, *Nature,* vol. 364, no. 6434, pp. 218-220.
DE DECKKER P., MOROS M., PERNER K. & JANSEN E. 2012 Influence of the tropics and southern westerlies on glacial interhemispheric asymmetry, *Nature Geoscience,* vol. 5, no. 4, pp. 266-269.
DULLER G. A. T. 2003 Distinguishing quartz and feldspar in single grain luminescence measurements, *Radiation measurements,* vol. 37, no. 2, pp. 161-165.
DULLER G. A. T. 2007 Luminescence Analyst. 3.24 ed. University of Wales, Aberystwyth: Aberystwyth Luminescence Research Laboratory.
DULLER G. A. T. 2008 Single-grain optical dating of Quaternary sediments: why aliquot size matters in luminescence dating, *Boreas,* vol. 37, pp. 598-612.
FLANNERY T. F. 1990 Pleistocene faunal loss: implications of the aftershock for Australia's past and future, *Archaeology in Oceania,* vol. 25, no. 2, pp. 45-55.
GALBRAITH R. & GREEN P. 1990 Estimating the component ages in a finite mixture, *International Journal of Radiation Applications and Instrumentation. Part D. Nuclear Tracks and Radiation Measurements,* vol. 17, no. 3, pp. 197-206.
GALBRAITH R. & LASLETT G. 1993 Statistical models for mixed fission track ages, *Nuclear tracks and radiation measurements,* vol. 21, no. 4, pp. 459-470.
GALBRAITH R. F. 2003 A simple homogeneity test for estimates of dose obtained using OSL, *Ancient TL,* vol. 21, no. 2, pp. 75-77.
GALBRAITH R. F., ROBERTS R. G., LASLETT G. M., YOSHIDA H. & OLLEY J. M. 1999 Optical dating of single and multiple grains of quartz from Jinmium Rock Shelter, Northern Australia: part I, experimental design and statistical models, *Archaeometry,* vol. 41, no. 2, pp. 339-364.
GANOPOLSKI A. & ROCHE D. M. 2009 On the nature of lead–lag relationships during glacial–interglacial climate transitions, *Quaternary Science Reviews,* vol. 28, no. 27, pp. 3361-3378.
GILLESPIE R. 1997 Burnt and unburnt carbon: dating charcoal and burnt bone from the Willandra Lakes, Australia, *Radiocarbon,* vol. 39, no. 3, pp. 239-250.
GUÉRIN G., JAIN M., THOMSEN K. J., MURRAY A. S. & MERCIER N. 2015 Modelling dose rate to single grains of quartz in well-sorted sand samples: The dispersion arising from the presence of potassium feldspars and implications for single grain OSL dating, *Quaternary Geochronology,* vol. 27, pp. 52-65.
HEINRICH H. 1988 Origin and consequences of cyclic ice rafting in the northeast Atlantic Ocean during the past 130,000 years, *Quaternary research,* vol. 29, no. 2, pp. 142-152.
HEIRI O., LOTTER A. F. & LEMCKE G. 2001 Loss on ignition as a method for estimating organic and carbonate content in sediments: reproducibility and comparability of results, *Journal of Paleolimnology,* vol. 25, pp. 101-110.
HESSE P. P. 1994 The record of continental dust from Australia in Tasman Sea sediments, *Quaternary Science Reviews,* vol. 13, no. 3, pp. 257-272.
HESSE P. P., MAGEE J. W. & VAN DER KAARS S. 2004 Late Quaternary climates of the Australian arid zone: a review, *Quaternary International,* vol. 118, pp. 87-102.
HUNTLEY D. J., GODFREY-SMITH D. I. & THEWALT M. L. W. 1987 Optical dating of sediments, *Nature,* vol. 313, pp. 105-107.
KELLEY R. A. & BAKER J. 1984 Geological development of North and South Stradbroke Islands and surround. Boolarong, Brisbane, Queensland, Australia.
KERSHAW A. 1974 A long continuous pollen sequence from north-eastern Australia.
KERSHAW A. 1976 A late Pleistocene and Holocene pollen diagram from Lynch's Crater, northeastern Queensland, Australia, *New Phytologist,* vol. 77, no. 2, pp. 469-498.
KERSHAW A., VAN DER KAARS S. & MOSS P. 2003 Late Quaternary Milankovitch-scale climatic change and variability and its impact on monsoonal Australasia, *Marine Geology,* vol. 201, no. 1, pp. 81-95.
KERSHAW A. P. 1986 Climactic change and Aboriginal burning in north-east Australia during the last two glacial/interglacial cycles, *Nature,* vol. 322, pp. 47-49.
KERSHAW A. P., MCKENZIE G. M., BROWN J., ROBERTS R. G. & VAN DER KAARS S. 2010 Beneath the peat: A refined pollen record from an interstadial at Caledonia Fen, highland eastern Victoria, Australia,

Altered Ecologies: Fire, Climate and Human Influence on Terrestrial Landscapes, Terra Australis, vol. 32, pp. 33-48.
KERSHAW A. P., MCKENZIE G. M., PORCH N., ROBERTS R. G., BROWN J., HEIJNIS H., ORR M. L., JACOBSEN G. & NEWALL P. R. 2007 A high-resolution record of vegetation and climate through the last glacial cycle from Caledonia Fen, southeastern highlands of Australia, *Journal of Quaternary Science,* vol. 22, no. 5, pp. 481-500.
LAMY F., GERSONDE R., WINCKLER G., ESPER O., JAESCHKE A., KUHN G., ULLERMANN J., MARTINEZ-GARCIA A., LAMBERT F. & KILIAN R. 2014 Increased Dust Deposition in the Pacific Southern Ocean During Glacial Periods, *Science,* vol. 343, pp. 403-407.
LIAN O. B. & ROBERTS R. G. 2006 Dating the Quaternary: progress in luminescence dating of sediments, *Quaternary Science Reviews,* vol. 25, no. 19–20, pp. 2449-2468.
LOPES DOS SANTOS R. A., DE DECKKER P., HOPMANS E. C., MAGEE J. W., METS A., SINNINGHE DAMSTÉ J. S. & SCHOUTEN S. 2013 Abrupt vegetation change after the Late Quaternary megafaunal extinction in southeastern Australia, *Nature Geoscience,* vol. 6, no. 8, pp. 627-631.
LOUTRE M.-F. & BERGER A. 2003 Marine Isotope Stage 11 as an analogue for the present interglacial, *Global and planetary change,* vol. 36, no. 3, pp. 209-217.
MILLER G. H., MAGEE J. W., JOHNSON B. J., FOGEL M. L., SPOONER N. A., MCCULLOCH M. T. & AYLIFFE L. K. 1999 Pleistocene extinction of Genyornis newtoni: human impact on Australian megafauna, *Science,* vol. 283, no. 5399, pp. 205-208.
MOONEY S., HARRISON S., BARTLEIN P., DANIAU A.-L., STEVENSON J., BROWNLIE K., BUCKMAN S., CUPPER M., LULY J. & BLACK M. 2011 Late Quaternary fire regimes of Australasia, *Quaternary Science Reviews,* vol. 30, no. 1, pp. 28-46.
MOSISCH T. D. & ARTHINGTON A. H. 2001 Polycyclic aromatic hydrocarbon residues in the sediments of a dune lake as a result of power boating, *Lakes & Reservoirs: Research and Management,* vol. 6, pp. 21-32.
MOSS P. T., TIBBY J., PETHERICK L., MCGOWAN H. & BARR C. 2013 Late Quaternary vegetation history of North Stradbroke Island, Queensland, eastern Australia, *Quaternary Science Reviews,* vol. 74, pp. 257-272.
MULLER J., KYLANDER M., WÜST R. A. J., WEISS D., MARTINEZ-CORTIZAS A., LEGRANDE A. N., JENNERJAHN T., BEHLING H., ANDERSON W. T. & JACOBSON G. 2008 Possible evidence for wet Heinrich phases in tropical NE Australia: the Lynch's Crater deposit, *Quaternary Science Reviews,* vol. 27, no. 5-6, pp. 468-475.
MURPHY B. P., WILLIAMSON G. J. & BOWMAN D. M. J. S. 2012 Did central Australian megafaunal extinction coincide with abrupt ecosystem collapse or gradual climate change?, *Global Ecology and Biogeography,* vol. 21, no. 2, pp. 142-151.
MURRAY A. S. & WINTLE A. G. 2000 Luminescence dating of quartz using an improved single-aliquot regenerative-dose protocol, *Radiation measurements,* vol. 32, no. 1, pp. 57-73.
MURRAY A. S. & WINTLE A. G. 2003 The single aliquot regenerative dose protocol: potential for improvements in reliability, *Radiation Measurements,* vol. 37, no. 4, pp. 377-381.
MYRBO A. & WRIGHT H. E. 2008 SOP: livingstone-bolivia. University of Minnesota: Limnological Research Center Core Facility.
OLLEY J., CAITCHEON G. G. & ROBERTS R. 1999 The origin of dose distributions in fluvial sediments, and the prospect of dating single grains from fluvial deposits using optically stimulated luminescence, *Radiation Measurements,* vol. 30, no. 2, pp. 207-217.
PETHERICK L. M., MOSS P. T. & MCGOWAN H. A. 2011 Climatic and environmental variability during the termination of the Last Glacial Stage in coastal eastern Australia: a review, *Australian Journal of Earth Sciences,* vol. 58, no. 6, pp. 563-577.
PICKETT J. W., THOMPSON C. H., KELLEY R. A. & ROMAN D. 1985 Evidence of High Sea Level during Isotope Stage 5c in Queensland, Australia, *Quaternary Research,* vol. 24, pp. 103-114.
PRESCOTT J. R. & HUTTON J. T. 1994 Cosmic ray contributions to dose rates for luminescence and ESR dating: large depths and long-term time variations, *Radiation measurements,* vol. 23, no. 2, pp. 497-500.
RAMSEY C. B. 1995 Radiocarbon Calibration and Analysis of Stratigraphy: The OxCal Program. Radiocarbon.
RIESER U. & WÜST R. A. J. 2010 OSL chronology of Lynch's Crater, the longest terrestrial record in NE-Australia, *Quaternary Geochronology,* vol. 5, no. 2-3, pp. 233-236.
ROBERTS R. G., KERSHAW P., MCKENZIE M., TURNEY C. S., CLEMENS S., BROWN J., MOSS P. & RULE S. 2003 Oxygen isotope stages 3 and 2 in Australia: High resolution palaeoenvironmental records from Lynch's Crater and Caledonia Fen.

RULE S., BROOK B. W., HABERLE S. G., TURNEY C. S., KERSHAW A. P. & JOHNSON C. N. 2012 The aftermath of megafaunal extinction: ecosystem transformation in Pleistocene Australia, *Science,* vol. 335, no. 6075, pp. 1483-6.
TEJAN-KELLA M. S., CHITTLEBOROUGH D. J., FITZPATRICK R. W., THOMPSON C. H., PRESCOTT J. R. & HUTTON J. T. 1990 Thermoluminescence Dating of Coastal Sand Dunes at Cooloola and North Stradbroke Island, Australia, *Australian Journal of Soil Research,* vol. 28, pp. 456-481.
THOMAS E. R., WOLFF E. W., MULVANEY R., JOHNSEN S. J., STEFFENSEN J. P. & ARROWSMITH C. 2009 Anatomy of a Dansgaard‐Oeschger warming transition: High‐resolution analysis of the North Greenland Ice Core Project ice core, *Journal of Geophysical Research,* vol. 114, no. D8.
THOMPSON C. H. 1992 Genesis of Podzols on Coastal Dunes in Southern Queensland. I. Field Relationships and Profile Morpholog, *Australian Journal of Soil Research,* vol. 30, no. 5, pp. 593-613.
THOMPSON C. H. & BOWMAN G. 1984 Subaerial denudation and weathering of vegetated coastal dunes in eastern Australia. Academic Press.
TIMMS B. 1986 The coastal dune lakes of eastern Australia. Limnology in Australia. pp. 421-432. Springer.
TURNEY C. S. M., KERSHAW A. P., JAMES S., BRANCH N., COWLEY J., FIFIELD L. K., JACOBSEN G. & MOSS P. 2006 Geochemical changes recorded in Lynch's Crater, Northeastern Australia, over the past 50 ka, *Palaeogeography, Palaeoclimatology, Palaeoecology,* vol. 233, no. 3-4, pp. 187-203.
VOELKER A. H. L. 2002 Global distribution of centennial-scale records for Marine Isotope Stage (MIS) 3: a database, *Quaternary Science Reviews,* vol. 21, pp. 1185–1212.
WALKER W., DAVIDSON G. R., LANGE T. & WREN D. 2007 Accurate lacustrine and wetland sediment accumulation rates determined from 14C activity of bulk sediment fractions, *Radiocarbon,* vol. 49, no. 2, pp. 983-992.
WARD W. T. 1978 Notes on the origin of Stradbroke Island, *Papers, Department of Geology, University of Queensland,* vol. 8, no. 2, pp. 97-104.
WARD W. T. 2006 Coastal dunes and strandplains in southeast Queensland: Sequence and chronology, *Australian Journal of Earth Sciences,* vol. 53, no. 2, pp. 363-373.
WINTLE A. G. & MURRAY A. S. 2006 A review of quartz optically stimulated luminescence characteristics and their relevance in single-aliquot regeneration dating protocols, *Radiation Measurements,* vol. 41, no. 4, pp. 369-391.
WOLFF E. W., CHAPPELLAZ J., BLUNIER T., RASMUSSEN S. O. & SVENSSON A. 2010 Millennial-scale variability during the last glacial: The ice core record, *Quaternary Science Reviews,* vol. 29, no. 21, pp. 2828-2838.
YANG J. & NEELIN J. D. 1993 Sea‐ice interaction with the thermohaline circulation, *Geophysical research letters,* vol. 20, no. 3, pp. 217-220.

APPENDIX A: TERMINOLOGY: ABBREVIATIONS, SYMBOLS AND UNITS

Abbreviations

OSL

OSL	Optically stimulated luminescence
CAM	Central Age Model
De	Equivalent Dose
DRT	Dose Recovery Test
FMM	Finite Mixture Model
IR	Infra-red (λ=700nm – 1mm)
MAM	Minimum Age Model
MG	Multiple Grain
OD	Over-dispersoin
PHx	Pre-heat condition
SAR	single-aliquot regeneration
SG	Single-grain
TL	Thermolumenescence

Other

ANSTO	Australian national nuclear research and development organisation
DO	Dansgaard–Oeschger
HRGS	High-resolution gamma ray spectrometer
ICP-MS	Inductively coupled plasma mass spectrometry
ICP-OES	Inductively coupled plasma optical emission spectrometry
LOI	Loss on ignition
MIS	Marine Isotope Stage
NSI	North Stradbroke Island
PVC	Polyvinyl chloride
THC	Thermohaline Circulation
ENSO	El Niño Southern Oscillation

Symbols

Units

Unit	Name	Meaning
Gy	Gray	The SI unit of energy absorbed from ionizing radiation
λ	Wavelength	The distance between successive crests of a wave, especially points in a sound wave or electromagnetic wave.

Radiation Types

Symbol	Name	Size Description	Penetration Ability
α	Alpha-particle	Consists of 2 protons and 2 neutrons and therefore has a positive charge.	few centimetres of air
β	Beta-particle	Is an electron and therefore has a negative charge.	few millimetres of aluminium
γ	Gamma Ray	No mass. It is at the small wavelength end of the electromagnetic spectrum	Penetrate through everything with an exponential decay

Definitions

Term	Definition	Units
Aliquot	A luminescence measurement consisting of multiple grains.	
Bleaching	Resetting of the 'clock' due to exposure to high temperatures or daylight.	
Dansgaard-Oeschger event	Rapid warming episodes, typically in a matter of decades, each followed by gradual cooling over a longer period	
Dose	The total amount of ionizing radiation absorbed by material.	Gy
Environmental Dose	Laboratory dose of beta or gamma radiation needed to induce luminescence equal to that acquired by sample subsequent to the most recent bleaching event (usually taken to be coincident with deposition).	Gy/ka
Dose Recovery Test	Involves irradiating a bleached sample with a known dose before heating at various temperatures to recover known dose. This test is used to determine the suitability of the chosen SAR preheat condition.	
Dose Regeneration Curve	The graph created when sensitivity corrected OSL is plotted against dose allowing for interpolation of the equivalent dose.	
El Niño Southern Oscillation	An irregularly periodical climate change caused by variations in sea surface temperatures over the tropical eastern Pacific Ocean, affecting much of the tropics and subtropics. The warming phase is known as El Niño and the cooling phase as La Niña	
Dose Rate	Dose per unit of time received by the sample while buried. It is the sum of all radiation types including α, β, γ and cosmic radiation at the study site since last bleaching event (deposition).	Gy/ka
Equivalent dose	Approximate equivalents of palaeodose	Gy
Heinrich Event	Large armadas of icebergs that break off from glaciers and traverse the North Atlantic	
Hole	A location lacking in charge in which trapped charges can recombine and luminesce.	
Intrinsic Scatter	Anomalous De values of grains of similar depositional age caused by heterogeneous ionizing radiation dispersion in sediments.	
Laurentide ice sheet	A massive sheet of ice that covered millions of square miles, including most of Canada and a large portion of the northern United States, multiple times during Quaternary glacial periods between c. 95,000 and c. 20,000 years.	
Luminescence	The emission of light from minerals, such as quartz and feldspar following an exposure to ionizing radiation and stimulation (thermal or optical) allowing recombination of charges.	
Optically stimulated	The umbrella term that includes luminescence resulting	

luminescence	from the stimulation by photos of any visible wavelength.	
Overdispersion	It is the amount of spread in a D_e dataset above and beyond that what can be expected for by the empirical D_e uncertainties.	%
Palaeodose	The total amount of ionizing radiation absorbed by the sample in nature.	Gy
Recombination	The instantaneous relocation of a trapped charge into a recombination centre of lower energy resulting in luminescence.	
Regenerative Dose (Regen-dose)	The recovered laboratory irradiated dose which is required to construct a luminescence vs dose growth curve.	
Regeneration method	The natural signal is bleached first and then doses are added to construct a luminescence vs. dose growth curve. The natural signal is then interpolated on to this regenerated growth curve to estimate the equivalent dose	
Sample Decay Curve	The exponentially relationship between photon counts and time during bleaching of a sample.	n/time
SAR protocol	A method developed by (Murray and Wintle 2000) for ensuring the reliability of measured De values. It consists of a test dose correction of sensitivity change and series of quality assurance checks a sample must pass or otherwise be rejected.	
Synthetic Aliquot	The production of an aliquot through averaging the dose response curves of one-hundred, single-grained samples.	
Test Dose	A constant laboratory dose given to a sample after measurement of the regenerative/natural dose to identify and corrected for any sensitivity changes in the quartz.	T_x
Thermohaline Circulation	A part of the large-scale ocean circulation that is driven by global density gradients created by surface heat and freshwater fluxes.	
Traps	A defect in the mineral lattice in which a charge can be stored (for seconds to millions of years) following exposure to ionizing radiation.	

Times Associated with Marine Isotope Stages

Marine Isotope Stage	Age (ka)	Notable Events
MIS 1	14	Continues to present
MIS 2	29	
MIS 3	57	Previous interglacial
MIS 4	71	
MIS 5a	82	
MIS 5b	78	Formation range of Welsby Lagoon
MIS 5c	96	
MIS 5d	109	
MIS 5e	123	
MIS 6	191	
MIS 7	243	
MIS 8	300	
MIS 9	337	
MIS 10	374	Possible Formation of North Stradbroke Island
MIS 11	424	
MIS 12	478	

APPENDIX B: SINGLE GRAIN REJECTION STATISTICS

Table B: The rejected single-grain statistic showing the classification of grains with respect to the single aliquot regenerative dose rejection criteria after measurement on the Risø machine.

	SG DRT WL2(1)		WL2(3)		WL2(7)		WL2(9)		WL2(11)	
	No. of grains	**% of grains**	**No. of grains**	**% of grains**	**No. of grains**	**% of grains**	**No. of grains**	**% of grains**	**No. of grains**	**% of grains**
Total measured grains	600		500		900		800		800	
SAR rejection criteria:										
Tn <3σ background	227	37.83	295	59.00	502	55.78	459	57.38	373	46.63
Recycling ratio ≠1 at ±2σ	40	6.67	11	2.20	34	3.78	25	3.13	19	2.38
0 Gy Lx/Tx >5% Ln/Tn	5	0.83	0	0.00	40	4.44	13	1.63	8	1.00
OSL-IR depletion ratios <1 at ±2σ [b]	22	3.67	14	2.80	22	2.44	26	3.25	15	1.88
Additional rejection criteria:										
Non-intersecting grains (Ln/Tn > dose response curve saturation)	7	1.17	0	0.00	13	1.44	2	0.25	0	0.00
Saturated grains (Ln/Tn ≈ dose response curve saturation)	8	1.33	0	0.00	3	0.33	6	0.75	10	1.25
Anomolous dose response / unable to perform Monte Carlo fit [a]	183	30.50	140	28.00	225	25.00	195	24.38	255	31.88
Sum of rejected grains	492	82.00	460	92.00	839	93.22	726	90.75	680	85.00
Sum of accepted grains	108	18.00	40	8.00	61	6.78	74	9.25	120	15.00

[a] includes grains which show linear dose response, grains with zero or negative changes in Li/Ti.
[b] grains yielding OSL-IR depletion ratios (Duller, 2003) of less than unity at 2σ

Table B: continued.

	WL2(12)		WL2(2)		WL2(1)		WL1(6)		WL1(7)	
	No. of grains	**% of grains**	**No. of grains**	**% of grains**	**No. of grains**	**% of grains**	**No. of grains**	**% of grains**	**No. of grains**	**% of grains**
Total measured grains	800		900		1200		700		600	
SAR rejection criteria:										
Tn <3σ background	459	57.38	370	41.11	485	40.42	306	43.71	285	47.50
Recycling ratio ≠1 at ±2σ	32	4.00	43	4.78	61	5.08	26	3.71	20	3.33
0 Gy Lx/Tx >5% Ln/Tn	23	2.88	34	3.78	8	0.67	0	0.00	0	0.00
OSL-IR depletion ratios <1 at ±2σ[b]	16	2.00	20	2.22	48	4.00	19	2.71	18	3.00
Additional rejection criteria:										
Non-intersecting grains (Ln/Tn > dose response curve saturation)	0	0.00	2	0.22	1	0.08	2	0.29	0	0.00
Saturated grains (Ln/Tn ≈ dose response curve saturation)	8	1.00	34	3.78	26	2.17	7	1.00	15	2.50
Anomolous dose response / unable to perform Monte Carlo fit[a]	183	22.88	277	30.78	432	36.00	209	29.86	156	26.00
Sum of rejected grains	721	90.13	780	86.67	1061	88.42	569	81.29	494	82.33
Sum of accepted grains	79	9.88	120	13.33	139	11.58	131	18.71	106	17.67

[a] includes grains which show linear dose response, grains with zero or negative changes in Li/Ti.
[b] grains yielding OSL-IR depletion ratios (Duller, 2003) of less than unity at 2σ

APPENDIX C: GENALYSIS DATA

Table C: Elemental concentrations provided through Genalysis for calculating dose rate. potassium, uranium and thorium concentrations were measured using ICP-MS and ICP-OES. The bottom shaded samples are control samples used by the laboratory.

Depth	Sample	K%	$K_{uncert.}$	U (ppm)	$U_{uncert.}$	Th (ppm)	$Th_{uncert.}$
380	2.3	0.010±	0.001	0.29±	0.03	0.46±	0.04
380	2.3[a]	0.010±	0.001	0.20±	0.02	0.37±	0.03
380	2.3[a]	0.010±	0.001	0.26±	0.03	0.38±	0.04
450	1.1	0.010±	0.001	0.26±	0.03	0.43±	0.04
480	2.5	0.020±	0.001	0.18±	0.02	0.81±	0.06
510	2.6	0.190±	0.001	0.90±	0.06	4.52±	0.27
550	1.2	0.220±	0.001	1.97±	0.13	8.41±	0.49
580	2.7	0.200±	0.001	1.65±	0.11	7.55±	0.45
610	2.8	0.230±	0.001	1.64±	0.11	7.10±	0.42
675	2.9	0.220±	0.001	1.52±	0.10	6.66±	0.39
750	1.4	0.270±	0.001	1.57±	0.10	7.11±	0.42
775	2.11	0.290±	0.001	1.58±	0.10	8.07±	0.48
815	2.12	0.350±	0.001	1.72±	0.11	8.55±	0.50
815	2.12	0.350±	0.001	1.71±	0.11	8.45±	0.50
850	1.5	0.320±	0.001	1.70±	0.11	8.15±	0.48
1258	2.2	0.040±	0.001	0.87±	0.06	3.37±	0.21
1270	1.7	0.020±	0.001	0.50±	0.04	2.28±	0.14
1258	1.6	0.060±	0.001	1.42±	0.09	3.86±	0.23
1270	2.1[a]	0.020±	0.001	0.36±	0.03	1.15±	0.08
1270	2.1[a]	0.010±	0.001	0.29±	0.03	1.12±	0.08
1270	2.1[a]	0.020±	0.001	0.42±	0.04	1.13±	0.08
1270	2.1	0.230±	0.001	1.64±	0.11	7.02±	0.42
	OREAS 624	0.950±	0.001	1.84±	0.12	4.16±	0.25
	SY-4	1.420±	0.001	0.76±	0.06	1.29±	0.09
	OREAS 100a	3.820±	0.001	131.06±	7.51	52.41±	3.01
	Control Blank	X	0.001	X	X	X	X

[a] duplicate samples for testing reproducibility.

APPENDIX D: OXCAL OUTPUT FOR "MEASURED" MODEL

Table Da: Confining parameters entered into the OxCal software for the Beysian modelling using ages from water contents directly measured through LOI.

		Measured Age (years)			
		1σ		2σ	
Sample	Depth (cm)	from	to	from	to
Top	0	1	0	1	0
N WL2(3)	380	27845	19734	31741	15837
N WL2(7)	580	53580	40586	59823	34343
N WL2(9)	675	50930	38312	56991	32251
N WL2(11)	775	65035	50077	72220	42892
N WL2(12)	815	58087	45145	64304	38928
N WL2(2)	1258	78090	67098	83370	61818
N WL1(7)	1270	78383	67773	83480	62676
Bottom	1272	-	-	-	-

Table Db: Modelled age data produced through OxCal including 1 and 2σ confidence intervals. Depths between 1-450 and 800-1250 have been omitted from the output.

	Modelled Age (years)			
	1σ		2σ	
Depth (cm)	from	to	from	to
450	29865	26015	34247	24221
452	30043	25997	34427	24255
453	30062	26134	34369	24352
454	30140	26228	34582	24468
455	30163	26291	34593	24435
457	30321	26322	34800	24578
458	30417	26422	34859	24637
459	30526	26472	35022	24746
460	30561	26540	34978	24843
462	30684	26617	35160	24872
463	30744	26741	35189	24959
464	30836	26777	35270	25004
466	30874	26849	35529	25197
467	31002	26914	35454	25201
468	31045	27030	35567	25307
469	31147	27070	35745	25384
471	31251	27153	35785	25383
472	31415	27247	35997	25498
473	31395	27315	35875	25643
474	31527	27352	36003	25750
476	31580	27492	36139	25721
477	31695	27572	36298	25851
478	31781	27624	36457	25862
480	31822	27671	36487	25979
481	31810	27794	36536	26052
482	32033	27843	36578	26177
483	32037	27907	36667	26153
485	32126	28026	36851	26296
486	32250	28051	37109	26318
487	32368	28178	36949	26334
488	32325	28219	37130	26539
490	32480	28335	37217	26545
491	32642	28363	37282	26651
492	32608	28396	37399	26748
494	32778	28556	37555	26862
495	32805	28624	37555	26958
496	32934	28701	37751	26963
497	33038	28699	37815	27010
499	33091	28817	37767	27238
500	33104	28944	37954	27273
501	33302	28914	38010	27292

502	33389	29059	38159	27376
504	33466	29141	38121	27418
505	33502	29233	38322	27529
506	33634	29298	38502	27552
508	33681	29315	38517	27685
509	33713	29405	38568	27768
510	33912	29541	38591	27807
511	34008	29585	38712	27940
513	33995	29674	38879	28012
514	34145	29719	38880	28110
515	34143	29718	38915	28206
518	34361	29998	39079	28329
519	34463	30028	39290	28351
520	34509	30011	39360	28516
522	34583	30198	39458	28624
523	34707	30315	39453	28667
524	34831	30310	39500	28842
525	34887	30476	39759	28832
527	35022	30521	39829	28957
528	35095	30620	39814	28968
529	35192	30593	39846	29090
530	35172	30691	40088	29120
532	35282	30851	40028	29257
533	35336	30842	40268	29241
534	35510	30983	40184	29391
536	35531	31017	40308	29465
537	35578	31121	40305	29536
538	35747	31208	40452	29618
539	35826	31305	40536	29602
541	35870	31359	40561	29770
542	36021	31411	40751	29874
543	35994	31549	40746	29954
544	36166	31588	40934	30033
546	36278	31661	41042	30033
547	36326	31703	41110	30193
548	36441	31845	41267	30296
551	36608	31980	41292	30445
552	36685	32055	41430	30444
553	36824	32097	41504	30563
555	36785	32171	41501	30640
556	36963	32304	41633	30686
557	36982	32337	41764	30806
558	37076	32317	41832	30872
560	37119	32486	41746	30956

561	37276	32574	41936	31045
562	37423	32636	42044	31053
563	37393	32701	42120	31183
565	37476	32824	42297	31314
566	37533	32811	42198	31441
567	37608	32956	42338	31586
569	37670	33011	42322	31487
570	37899	33122	42347	31661
571	37953	33193	42475	31679
572	37945	33184	42610	31841
574	38053	33320	42625	31821
575	38205	33404	42609	32053
576	38284	33481	42846	32017
577	38389	33535	42844	32045
579	38699	33621	43069	32176
580	38611	33717	43398	32230
581	38740	33778	43621	32381
583	38766	33880	43638	32331
584	38831	33882	43634	32467
585	38938	34010	43639	32605
586	39031	34084	43826	32710
588	39080	34172	43892	32717
589	39186	34206	43913	32782
590	39225	34091	43950	32829
591	39291	34374	44034	32844
593	39420	34509	44047	32991
594	39411	34541	44335	33115
595	39491	34673	44297	33133
597	39558	34672	44357	33135
598	39574	34739	44448	33265
599	39816	34947	44423	33381
600	39762	34937	44496	33482
602	39921	35030	44544	33498
603	40053	35121	44657	33436
604	39941	35135	44661	33605
605	40089	35188	44740	33767
607	40224	35361	44837	33851
608	40213	35353	44959	33860
609	40286	35519	45058	33982
611	40389	35580	45065	34021
612	40513	35692	45100	34116
613	40552	35721	45140	34136
614	40622	35828	45187	34264
616	40843	35921	45361	34379

617	40869	35993	45350	34343
619	41042	36110	45518	34505
621	41133	36238	45554	34610
622	41041	36238	45644	34644
623	41327	36370	45797	34781
625	41293	36317	45804	34777
626	41401	36444	45860	34921
627	41552	36562	45921	34923
628	41564	36689	46102	35017
630	41627	36706	46067	35058
631	41668	36859	46195	35256
632	41852	36889	46278	35280
633	41970	36971	46356	35389
635	42009	37027	46369	35393
636	41999	37131	46363	35534
639	42260	37250	46553	35710
640	42324	37314	46633	35784
641	42341	37377	46680	35801
642	42431	37561	46757	35960
644	42516	37595	46899	35970
645	42512	37654	46883	36027
646	42695	37733	46972	36150
647	42774	37811	47059	36128
649	42854	37919	47069	36348
650	42936	38047	47154	36331
651	43067	37964	47155	36496
653	43115	38097	47324	36424
654	43075	38207	47419	36645
655	43294	38334	47357	36730
656	43313	38266	47460	36729
658	43405	38455	47465	36791
659	43457	38551	47585	36923
660	43503	38569	47608	36865
661	43614	38675	47693	37074
663	43961	38785	47776	37140
664	43715	38811	47866	37207
665	43993	38954	47908	37284
667	43984	38986	47881	37403
668	44068	39026	47975	37397
669	44090	39150	48233	37508
670	44112	39115	48042	37606
672	44160	39332	48111	37670
673	44290	39347	48243	37753
674	44318	39451	48246	37751

675	44410	39485	48706	37893
677	44713	39667	48629	37967
678	44729	39642	48851	38043
679	44852	39712	48959	38107
681	44936	39734	48988	38155
682	44911	39718	49077	38279
683	45069	39956	49160	38260
684	45026	40025	49112	38395
686	45205	40222	49209	38433
687	45157	40236	49196	38568
688	45447	40225	49332	38577
689	45323	40466	49445	38650
691	45408	40523	49513	38732
692	45464	40574	49474	38826
693	45611	40650	49646	38925
695	45709	40679	49714	38996
696	45857	40819	49864	39030
697	45802	40882	49795	39098
698	45929	40932	49885	39180
700	45962	40977	49995	39260
701	46016	41130	50056	39177
702	46100	41130	50172	39356
703	46214	41245	50220	39459
705	46300	41320	50296	39501
706	46456	41409	50310	39641
707	46482	41423	50405	39664
709	46541	41579	50521	39764
711	46720	41731	50591	39855
712	46868	41802	50692	39956
714	46859	41874	50765	40041
715	46954	41900	50805	40105
716	47094	42010	50941	40145
717	47032	42116	50926	40244
719	47154	42193	51029	40307
720	47244	42255	51096	40359
721	47274	42308	51196	40437
722	47390	42452	51370	40465
724	47462	42490	51407	40590
725	47571	42540	51437	40668
726	47563	42577	51506	40788
728	47662	42696	51596	40850
729	47746	42737	51683	40857
730	47882	42860	51677	40965
731	47979	42915	51842	40978

733	47977	42981	51915	41176
734	48128	43059	51992	41170
735	48108	43170	51982	41264
736	48216	43247	52029	41349
738	48325	43292	52159	41439
739	48421	43348	52218	41478
740	48477	43497	52294	41508
742	48468	43506	52296	41591
743	48676	43558	52478	41814
744	48732	43722	52557	41777
745	48831	43727	52495	41863
747	48821	43877	52623	41928
748	48899	43879	52709	41871
749	48959	43945	52750	42119
750	49091	44066	52867	42166
752	49321	44098	53002	42158
753	49323	44209	52924	42260
754	49369	44362	53040	42362
756	49402	44409	53127	42450
757	49478	44461	53130	42412
758	49615	44582	53234	42542
759	49584	44652	53322	42626
761	49710	44701	53422	42677
762	49831	44757	53361	42832
763	49973	44825	53484	42862
764	49902	44937	53587	42973
766	50024	44995	53588	42957
767	50114	44997	53617	43084
768	50171	45147	53733	43157
770	50351	45155	53842	43259
771	50303	45299	53869	43378
772	50355	45316	53943	43331
773	50564	45383	53877	43405
775	50648	45482	54169	43477
776	50674	45627	54334	43651
777	50846	45696	54333	43720
778	50825	45767	54410	43815
780	50950	45845	54539	43890
781	51015	45857	54517	43970
782	51186	46004	54693	43975
784	51192	46071	54649	44072
785	51225	46134	54823	44175
786	51456	46150	54813	44194
787	51398	46320	54931	44204
789	51463	46343	54998	44322
790	51539	46441	55014	44409
791	51660	46525	55133	44495
792	51732	46516	55193	44476
794	51752	46669	55232	44604
795	51835	46776	55310	44621
796	52018	46833	55320	44837
798	52009	46933	55375	44785
799	52116	47005	55499	44871
800	52120	47013	55539	44980
1250	79390	71808	81952	68929
1252	79469	72174	82080	69067
1253	79623	71949	82194	69209
1254	79645	72025	82140	69116
1255	80003	72056	82239	69349
1257	79796	72223	82343	68888
1258	79949	72496	82405	69475
1259	79947	72599	82610	69473
1261	79991	72886	82741	69475
1262	80100	72840	82817	69486
1263	80175	72947	82968	69619
1264	80096	72973	83031	69754
1266	80332	73031	83082	69851
1267	80419	73046	83134	69477
1268	80477	72948	83220	69990
1269	80423	72785	83295	69900
1271	80792	73073	83376	70436

APPENDIX E: OXCAL OUTPUT FOR "COMPACTION" MODEL

Table Ea: Confining parameters entered into the OxCal software for the Beysian modelling using ages from water contents compaction corrected from measurements through LOI.

		Measured Age (years)			
		1σ		2σ	
Sample	Depth (cm)	from	to	from	to
Top	0	1	0	1	0
N WL2(3)	380	32229	22197	37049	17377
N WL2(7)	580	74419	53221	84602	43038
N WL2(9)	675	82290	57584	94159	45715
N WL2(11)	775	98583	70865	111899	57550
N WL2(12)	815	96670	69296	109821	56145
N WL2(2)	1258	96191	81161	103413	73940
N WL1(7)	1270	111556	93265	120342	84478
Bottom	1272	-	-	-	-

Table Eb: Modelled age data produced through OxCal including 1 and 2σ confidence intervals. Depths between 1-450 and 800-1250 have been omitted from the output.

	Modelled Age (years)			
	1σ		2σ	
Depth (cm)	from	to	from	to
450	39471	33048	46968	28663
452	39695	33081	47267	28795
453	39817	33180	47178	29073
454	39969	33277	47441	29296
455	40046	33343	47482	29368
457	40168	33367	47936	29466
458	40150	33510	48021	29492
459	40430	33706	48100	29601
460	40461	33795	48253	29756
462	40677	33841	48551	29813
463	40685	34003	48590	29934
464	40895	34096	48667	30070
466	40920	34214	49039	30057
467	41166	34164	49151	30213
468	41179	34321	49339	30439
469	41326	34444	49413	30412
471	41425	34576	49738	30767
472	41468	34708	49845	30702
473	41649	34796	50176	30844
474	41745	34873	50313	31128
476	41920	34873	50317	31196
477	41939	34974	50688	31139
478	42196	35082	50805	31359
480	42294	35220	51072	31443
481	42332	35342	51234	31590
482	42612	35570	51095	31524
483	42632	35504	51292	31773
485	42852	35640	51422	31955
486	42887	35759	51707	32127
487	43047	35870	51796	32083
488	43017	36035	52014	32419
490	43291	36093	52178	32337
491	43307	36062	52254	32518
492	43474	36243	52659	32641
494	43556	36275	52566	32777
495	43703	36435	52806	32746
496	43875	36607	52888	32904
497	43825	36603	53062	33223
499	44031	36721	53486	33124
500	44162	36836	53403	33317
501	44259	36965	53313	33529
502	44479	36937	53760	33587

504	44542	37199	54015	33688
505	44608	37237	54423	33836
506	44748	37377	54173	33845
508	44856	37458	54603	34150
509	44983	37559	54664	34052
510	45129	37568	54661	34504
511	45253	37588	54902	34535
513	45457	37749	54946	34646
514	45461	38000	55087	34700
515	45661	38048	55147	34834
516	45879	38147	55416	34973
518	45852	38193	55325	35257
519	45984	38378	55644	35207
520	46107	38466	55696	35403
522	46153	38570	55730	35377
523	46276	38426	56165	35612
524	46492	38741	56084	35645
525	46530	38719	56293	35923
527	46609	38932	56632	35933
528	46732	38996	56546	35902
529	46869	39148	56571	36184
530	47099	39039	56848	36309
532	47272	39344	57040	36436
533	47374	39459	57035	36623
534	47440	39507	57079	36668
536	47551	39557	57117	36830
537	47779	39737	57309	36883
538	47891	39752	57394	37019
539	47985	39844	57668	37164
541	48297	39892	58041	37108
542	48058	40055	58113	37203
543	48183	40232	57725	37246
544	48479	40312	58162	37572
546	48485	40350	58146	37747
547	48718	40454	58448	37708
548	48872	40521	58635	37922
550	48884	40566	58707	37956
551	49037	40737	58801	38061
552	49230	40767	58883	38240
553	49295	41093	58988	38318
555	49296	40907	59367	38575
556	49387	41142	59113	38627
557	49687	41298	59442	38644
558	49812	41176	59401	38917

560	49933	41562	59525	38918
561	49944	41634	59627	39117
562	50076	41626	59659	39173
563	50256	41808	59996	39231
565	50263	41792	59903	39177
566	50485	41930	60353	39454
567	50670	42116	60072	39612
569	51013	42276	60373	39792
570	50993	42364	60193	39842
571	51072	42425	60445	39824
572	51348	42509	60481	40020
574	51186	42641	60690	40212
575	51569	42734	60655	40249
576	51495	42785	60890	40378
577	51582	42662	61016	40490
579	51650	43125	61221	40708
580	52118	42890	62284	41030
581	52441	42982	62669	41045
583	52588	43320	62737	41322
584	52513	43172	62643	41138
585	52567	43234	62950	41358
586	52914	43653	62822	41248
588	53030	43492	62924	41479
589	52893	43880	62860	41497
590	52943	43893	63159	41662
591	53056	44052	63122	41745
593	53280	44184	63289	41836
594	53240	44251	63552	41951
595	53412	44232	63691	42097
597	53470	44428	63538	42008
598	53751	44184	63783	42217
599	53806	44611	63931	42202
600	53951	44576	64115	42458
602	53850	44760	64048	42599
603	54073	44993	64226	42642
604	54255	45081	64163	42746
605	54294	45194	64408	42804
607	54452	45214	64563	42794
608	54642	45323	64634	42928
609	54690	45434	64692	42947
611	54845	45277	64844	43126
612	54978	45653	64793	43215
613	55062	45627	65049	43355
614	55007	45811	65039	43410

616	55250	45797	65312	43496
617	55334	46101	65117	43714
618	55424	46179	65564	43659
619	55663	46053	65459	43857
621	55786	46342	65529	43966
622	55763	46380	65684	43930
623	55737	46581	65784	43998
625	55828	46623	65946	44170
626	56139	46562	66091	44354
627	56270	46759	66123	44385
628	56417	46730	66212	44526
630	56394	47035	66250	44549
631	56586	47103	66356	44738
632	56688	47190	66534	44855
633	56783	47202	66476	44803
635	56797	47436	66776	44908
636	56953	47506	66743	45185
637	57175	47631	66861	45171
639	57094	47621	67128	45190
640	57270	47831	67045	45397
641	57461	47926	67157	45320
642	57451	48053	67272	45487
644	57552	48102	67545	45555
645	57703	48249	67535	45660
646	57874	48292	67619	45886
647	57880	48428	67589	45876
649	58085	48481	67802	46074
650	58355	48660	67737	46179
651	58254	48677	68055	46091
653	58386	48777	68279	46266
654	58487	48926	68077	46304
655	58812	49009	68255	46591
656	58695	49058	68325	46671
658	58749	49179	68400	46632
659	58668	49201	68282	46770
660	59051	49407	68413	46871
661	59118	49431	68680	46856
663	59385	49565	68876	47025
664	59241	49654	68916	47145
665	59735	49746	69134	47495
667	59638	49861	69062	47329
668	59709	49913	69090	47363
669	59751	50078	69060	47499
670	59829	50205	69167	47838

672	60019	50220	69363	47963
673	60212	50387	69568	47797
674	60015	50420	69731	47933
675	60502	50494	70308	48470
677	60513	50602	70385	48526
678	60917	50342	70515	48515
679	60778	50778	70652	48671
681	60882	50864	70784	48631
682	60929	50968	70900	48827
683	61065	51135	70914	48774
684	61089	51306	71220	48676
686	61303	51288	71215	49125
687	61626	51439	71209	48774
688	61379	51462	71344	48985
689	61620	51557	71265	49256
691	61739	51784	71488	49306
692	61920	51827	71492	49636
693	61996	51887	71479	49760
695	62321	51968	71673	49617
696	62338	51962	71865	49836
697	62234	52163	71958	49888
698	62440	52268	71926	49957
700	62383	52386	71975	49911
701	62614	52549	72122	50203
702	62855	52604	72250	50051
703	62806	52745	72576	50483
705	63336	52885	72390	50369
706	62939	52920	72674	50396
707	63213	53020	72563	50621
709	63188	53033	72812	50713
710	63338	53161	72855	50595
711	63200	53437	72931	50868
712	63344	53361	72993	50664
714	63456	53555	72997	51156
715	63830	53728	73203	51200
716	63725	53634	73237	51063
717	64029	53742	73383	51402
719	64202	53801	73521	51287
720	64239	53883	73460	51575
721	64055	53952	73566	51683
722	64182	54211	73812	51814
724	64288	54415	73957	51906
725	64421	54434	73873	51539
726	64947	54534	73956	51984

728	64804	54706	74096	52124
729	64766	54764	74306	51941
730	64772	54869	74359	52336
731	64953	54949	74182	52060
733	65230	55105	74552	52565
734	65243	55013	74655	52575
735	65480	55290	74654	52672
736	65293	55375	74684	52824
738	65420	55309	74641	52961
739	65632	55511	74845	52954
740	65745	55652	74955	53100
742	65702	55702	75109	53098
743	65973	55871	75392	53316
744	66026	55964	75473	53246
745	66050	56125	75384	53557
747	66302	56148	75364	53522
748	66274	56211	75604	53636
749	66651	56392	75564	53811
750	66546	56428	75692	53831
752	66653	56548	75598	53876
753	66716	56634	75827	54032
754	66942	56827	76008	54170
756	66992	56774	76003	54322
757	67094	56968	76012	54246
758	67009	56819	76400	54425
759	67334	57185	76316	54543
761	67332	57259	76363	54641
762	67391	57426	76547	54702
763	67645	57341	76447	54844
764	67753	57530	76359	54914
766	67703	57594	76743	55021
767	67916	57795	76717	55148
768	68045	57691	76743	54748
770	68133	57911	76905	55324
771	68206	57984	76885	55444
772	68230	58215	76983	55501
773	68557	58186	77033	55599
775	68525	58282	77190	55714
776	68812	58373	77711	55773
777	68905	58443	77945	55956
778	68960	58559	78023	56022
780	68962	58788	78057	56033
781	69151	58745	78026	56141
782	69268	58905	78051	56221

784	69210	58934	78194	56313
785	69586	59051	78349	56429
786	69585	59285	78293	56494
787	69498	59260	78295	56538
789	69655	59398	78620	56669
790	69794	59596	78479	56677
791	70095	59592	78743	56891
792	70009	59746	78806	56897
794	70151	59785	78810	57063
795	70324	59905	78840	57117
796	70338	60125	78860	57223
798	70442	60029	78914	57368
799	70388	60145	79196	57357
800	70640	60331	79249	57389
1250	104481	92540	108301	88370
1252	104666	93138	108356	88318
1253	104728	93207	108360	88656
1254	104695	92845	108549	88585
1255	104962	93738	108622	89094
1257	104987	93665	108785	89053
1258	105591	93662	109122	89239
1259	105218	93679	109320	89360
1261	105332	93277	109545	89475
1262	105444	93956	110144	89565
1263	105423	94135	110265	89602
1264	105634	94282	110373	89674
1266	105595	94300	110469	89608
1267	105886	94449	110568	89675
1268	105971	94298	110555	89808
1269	106111	94039	110589	89902
1271	107407	92061	110061	89963

APPENDIX F: MULTI-GRAIN ALUQUOT DATA

Table F: Multi-grain aliquot statistical data used in comparison with respective single-grain measurements.

Sample	Depth (m)	No of grains per aliquot	Accepted aliquots/measured	Over-dispersion (%)	CAM De (Gy)	CAM age (ka)
Welsby Lagoon Core 2						
WL15/2 (03)	3.8	~100	3/5	89.2 ± 36.5	4.842 ± 2.496	37.12 ± 20.13
WL15/2 (07)	5.8	~100	5/9	41.3 ± 13.1	9.657 ± 1.786	69.42 ± 17.03
WL15/2 (09)	6.75	~100	6/8	22.6 ± 6.6	18.194 ± 1.685	133.85 ± 24.75
WL15/2 (11)	7.75	~100	7/8	16.0 ± 4.3	14.908 ± 0.910	95.55 ± 16.27
WL15/2 (12)	8.15	~100	3/8	20.8 ± 8.7	13.782 ± 1.674	81.36 ± 16.29
WL15/2 (02)	12.585	~100	6/9	15.1 ± 4.4	26.596 ± 1.650	99.33 ± 9.99
WL15/2 (01)	12.701	~100	6/12	15.3 ± 4.5	23.485 ± 1.483	27.34 ± 1.98
Welsby Lagoon Core 1						
WL15/1 (06)	12.58	~100	5/7	6.3 ± 2.2	26.200 ± 0.769	108.05 ± 10.64
WL15/1 (07)	12.695	~100	5/6	11.6 ± 3.8	33.574 ± 1.774	165.63 ± 17.10